PROPAGATION OF MULTIWAVELENGTH LASER RADIATION THROUGH ATMOSPHERIC TURBULENCE

J. Richard Kerr, et al

Oregon Graduate Center

Prepared for:

Rome Air Development Center

November 1974

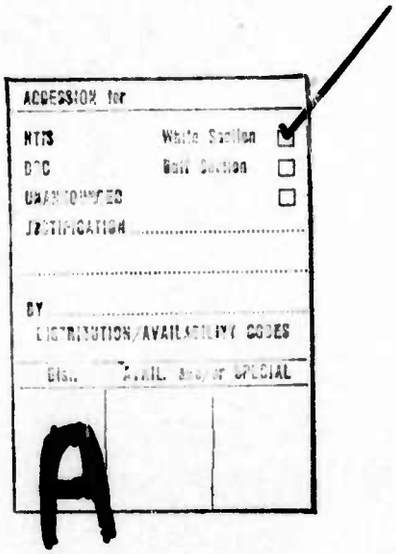

Do not return this copy. Retain or destroy.

UNCLASSIFIED

SECURITY CLASSIFICATION OF THIS PAGE *(When Data Entered)*

REPORT DOCUMENTATION PAGE	READ INSTRUCTIONS BEFORE COMPLETING FORM
1. REPORT NUMBER RADC-TR-74-320	2. GOVT ACCESSION NO.
	3. RECIPIENT'S CATALOG NUMBER AD/A-003340
4. TITLE *(and Subtitle)* Propagation of Multiwavelength Laser Radiation Through Atmospheric Turbulence	5. TYPE OF REPORT & PERIOD COVERED Final Technical Report 1 Dec 73 - 1 Sep 74
	6. PERFORMING ORG. REPORT NUMBER
7. AUTHOR(s) J. Richard Kerr Richard A. Elliott Philip A. Pincus Myung H. Lee	8. CONTRACT OR GRANT NUMBER(s) F30602-74-C-0082
9. PERFORMING ORGANIZATION NAME AND ADDRESS Oregon Graduate Center 19600 N. W. Walker Road Beaverton Oregon 97005	10. PROGRAM ELEMENT, PROJECT, TASK AREA & WORK UNIT NUMBERS 62301E 12790212
11. CONTROLLING OFFICE NAME AND ADDRESS Defense Advanced Research Projects Agency 1400 Wilson Blvd Arlington VA 22209	12. REPORT DATE November 1974 13. NUMBER OF PAGES 67
14. MONITORING AGENCY NAME & ADDRESS*(if different from Controlling Office)* Rome Air Development Center (OCSE) ATTN: Capt. Darryl P. Greenwood Griffiss AFB NY 13441	15. SECURITY CLASS. *(of this report)* UNCLASSIFIED 15a. DECLASSIFICATION/DOWNGRADING SCHEDULE N/A

16. DISTRIBUTION STATEMENT *(of this Report)*

Approved for public release; distribution unlimited.

17. DISTRIBUTION STATEMENT *(of the abstract entered in Block 20, if different from Report)*

Same

18. SUPPLEMENTARY NOTES

None

19. KEY WORDS *(Continue on reverse side if necessary and identify by block number)*

Propagation
Turbulence
Atmospheric Optics
Scintillation

20. ABSTRACT *(Continue on reverse side if necessary and identify by block number)*

This report reviews in detail our progress on understanding the short-term statistics of microthermal turbulence fluctuations and optical/infrared scintillations, and their interrelationship. A complete analytical understanding of microthermal and scintillation data-spread and confidence intervals has been achieved, including the effects of microthermal-envelope probability distributions, integral scales, varying averaging times, and turbulence intermittency. A practical definition and model of intermittent turbulence is given and it is

DD FORM 1 JAN 73 1473 EDITION OF 1 NOV 65 IS OBSOLETE

UNCLASSIFIED

SECURITY CLASSIFICATION OF THIS PAGE *(When Data Entered)*

shown that the usual mathematical techniques may be applied. The fundamental determining factor in data spread is shown to be the two-point correlation of the microthermal envelope fluctuations along the propagation path, with applications to the short-term performance of imaging as well as illumination systems. Supporting data are given.

As an addendum to the preceding report on this program, which deals with turbulence effects on finite aperture laser illumination systems, the effective aperture size of an arbitrarily truncated gaussian beam is derived. In addition, it is shown from the Huygens-Fresnel formulation that the normalized variance of target irradiance for a large transmitter or small coherence scale (ρ_o) is unity, in agreement with recent data and physical reasonings.

PROPAGATION OF MULTIWAVELENGTH LASER RADIATION THROUGH ATMOSPHERIC TURBULENCE

J. Richard Kerr
Richard A. Elliott
Philip A. Pincus
Myung H. Lee

Contractor: Oregon Graduate Center
Contract Number: F30602-74-C-0082
Effective Date of Contract: 1 December 1973
Contract Expiration Date: 1 September 1974
Amount of Contract: $64,715.00
Program Code Number: 4E20
Period Covered: 1 Dec 73 - 1 Sep 74

Principal Investigator: Dr. J. Richard Kerr
Phone: 503 645-1121

Project Engineer: Capt. Darryl P. Greenwood
Phone: 315 330-3145

This research was supported by the Defense Advanced Research Projects Agency of the Department of Defense and was monitored by Capt. Darryl P. Greenwood, RADC (OCSE), GAFB NY 13441 under Contract F30602-74-C-0082, Job Order No. 12790212.

This report has been reviewed by the RADC Information Office (OI) and is releasable to the National Technical Information Service (NTIS). At NTIS it will be available to the general public, including foreign nations.

This technical report has been reviewed and is approved for publication.

Darryl P. Greenwood

RADC Project Engineer

Summary

This report reviews in detail our progress on understanding the short-term statistics of microthermal turbulence fluctuations and optical/infrared scintillations, and their interrelationship. A complete analytical understanding of microthermal and scintillation data-spread and confidence intervals has been achieved, including the effects of microthermal-envelope probability distributions, integral scales, varying averaging times, and turbulence intermittency. A practical definition and model of intermittent turbulence is given, and it is shown that the usual mathematical techniques may be applied. The fundamental determining factor in data spread is shown to be the two-point correlation of the microthermal envelope fluctuations along the propagation path, with applications to the short-term performance of imaging as well as illumination systems. Supporting data are given.

As an addendum to the preceding report on this program, which deals with turbulence effects on finite aperture laser illumination systems, the effective aperture size of an arbitrarily truncated gaussian beam is derived. In addition, it is shown from the Huygens-Fresnel formulation that the normalized variance of target irradiance for a large transmitter or small coherence scale (ρ_o) is unity, in agreement with recent data and physical reasonings.

TABLE OF CONTENTS

I. INTRODUCTION

This report describes progress on two projects, one in detail. In the next section (II), we describe at length the theoretical and preliminary experimental results of our efforts on the short-term statistics of turbulence and optical/infrared propagation. In the following section (III), some recent developments in the work on finite, wander-tracking laser illumination systems are briefly discussed.

II. SHORT-TERM TURBULENCE AND PROPAGATION STATISTICS

Significant conceptual, analytical, and experimental progress has been made on the description of the short-term statistics of turbulence and scintillation phenomena. In the present section, this progress will be reviewed in a largely self-contained manner, such that little or no familiarity with earlier reports[1] will be assumed on the part of the reader.

The basic topics of interest here are the description of basic microthermal fluctuations, the short-term statistics of appropriate averaged quantities, short-term measures of propagation effects and their relationship to the microthermal quantities, the influence of the choice of averaging times, intermittency of turbulence, and related items. These aspects will be discussed in the following subsections.

A. Statistics of the Basic Microthermal Fluctuations

The basic microthermal fluctuations associated with the turbulence effects of interest are known to be characterized by probability distributions which differ markedly from normality. In particular, if the temperature difference fluctuations between two probes (ΔT_{12}) are observed, where the probe separation is within the inertial subrange, the distribution is symmetric with a *flatness factor which may be as high as 40, compared to a value of 3 for the normal distribution. A typical

---

*The flatness factor is defined as the ratio of the fourth central moment to the square of the second central moment. The skewness is the squared third central moment divided by the cubed second central moment.

---

1. J. R. Kerr, "Propagation of Multiwavelength Laser Radiation Through Atmospheric Turbulence", RADC-TR-73-322, August, 1973. (AD769 792)

record of such fluctuations is shown in Fig. 1, and the probability distribution in Fig. 2, exhibiting a flatness factor in this case of 8. Physically, this exaggerated tail on the probability distribution relates to occasional fluctuations of extreme magnitude ("small-scale intermittency"), and is fundamental to turbulence phenomena.[2]

Although the above distribution is basically amorphous, we are more interested in an appropriate measure of the strength of turbulence, and therefore in the statistics of an appropriate average or smoothed quantity. This quantity is the (short-term) average of the square of the temperature-difference fluctuations, which we obtain here through digital low-pass filtering techniques.

Theoretical treatments[3] have predicted that non-negative, differential (or finite-difference) turbulence variables will exhibit log normal behavior when averaged over a spatial or temporal scale corresponding to the inertial subrange. Probability distributions of the (log) squared temperature difference fluctuations are shown in Fig. 3 for several smoothing or averaging scales, and log normality is verified except at small values of $(\Delta T_{12})^2$. This departure at small values is not due to instrumental noise, and has been observed in nearly all experiments on turbulent temperature and velocity fluctuations. The apparent effect of the inner scale of turbulence is also seen in Fig. 3.

As the averaging time or scale size is increased, one expects, based on the central limit theorem, to observe the approach of the distribution to normality. This approach is conveniently displayed on a "beta diagram",[4] which is a plot of the flatness factor (β_2) vs. the skewness (β_1). The beta diagram for $(\Delta T_{12})^2$ over a range of averaging times is shown in Fig. 4. Also shown is the point ($\beta_2 = 3$, $\beta_1 = 0$) corresponding to normality, and the line representing the family of log normal distributions. The displacements of the experimental points from the log normal line, especially at small averaging times, is due in part to the inability to measure the higher moments of a

---

2. A.M.Yaglom, Soviet Physics-Doklady 11, 26-29, July 1966.
3. A.S.Gurvich and A.M.Yaglom, Phys. of Fluids Suppl., Boundary Layers and Turbulence, 10, Part II, S59-S65 (1967).
4. G.J. Hahn and S.S.Shapiro, Statistical Models in Engineering, Wiley & Sons, 197 (1967).

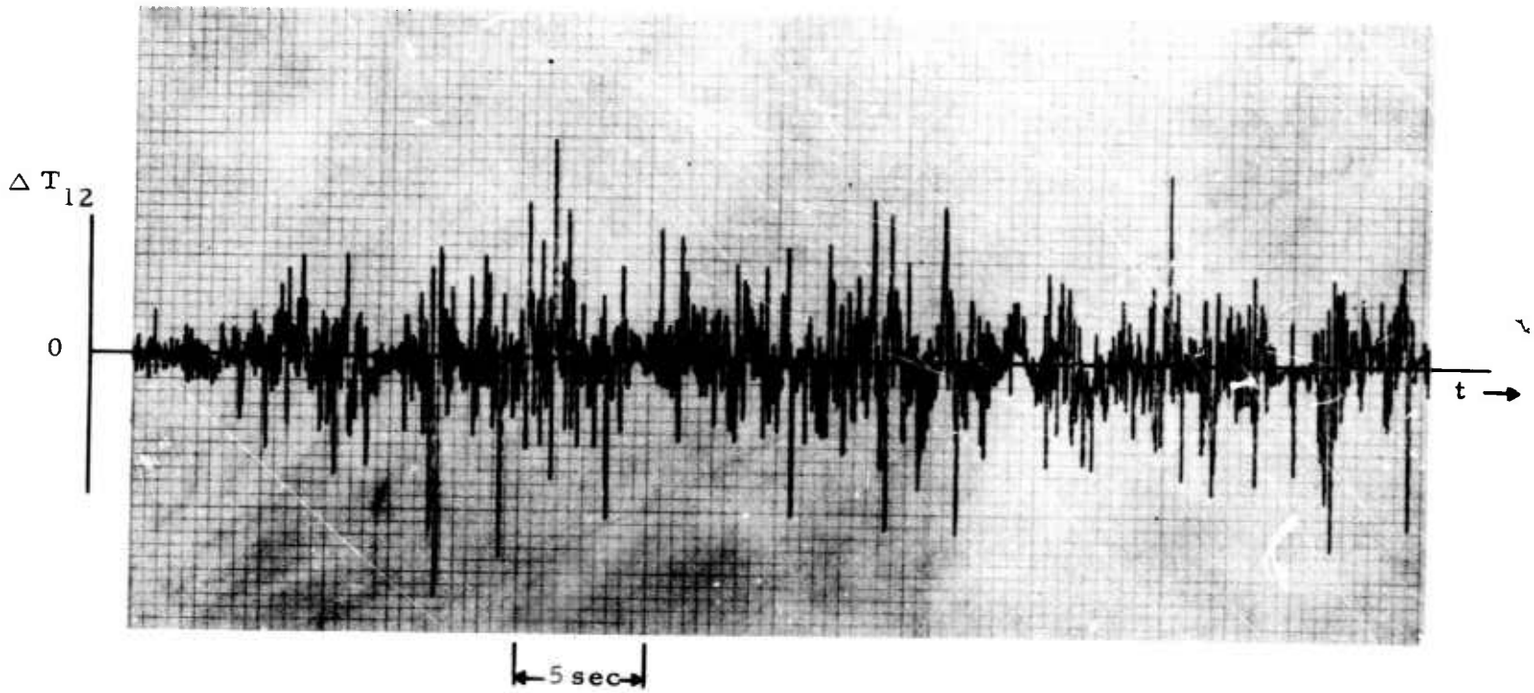

Figure 1. Typical two-probe temperature-difference fluctuations.

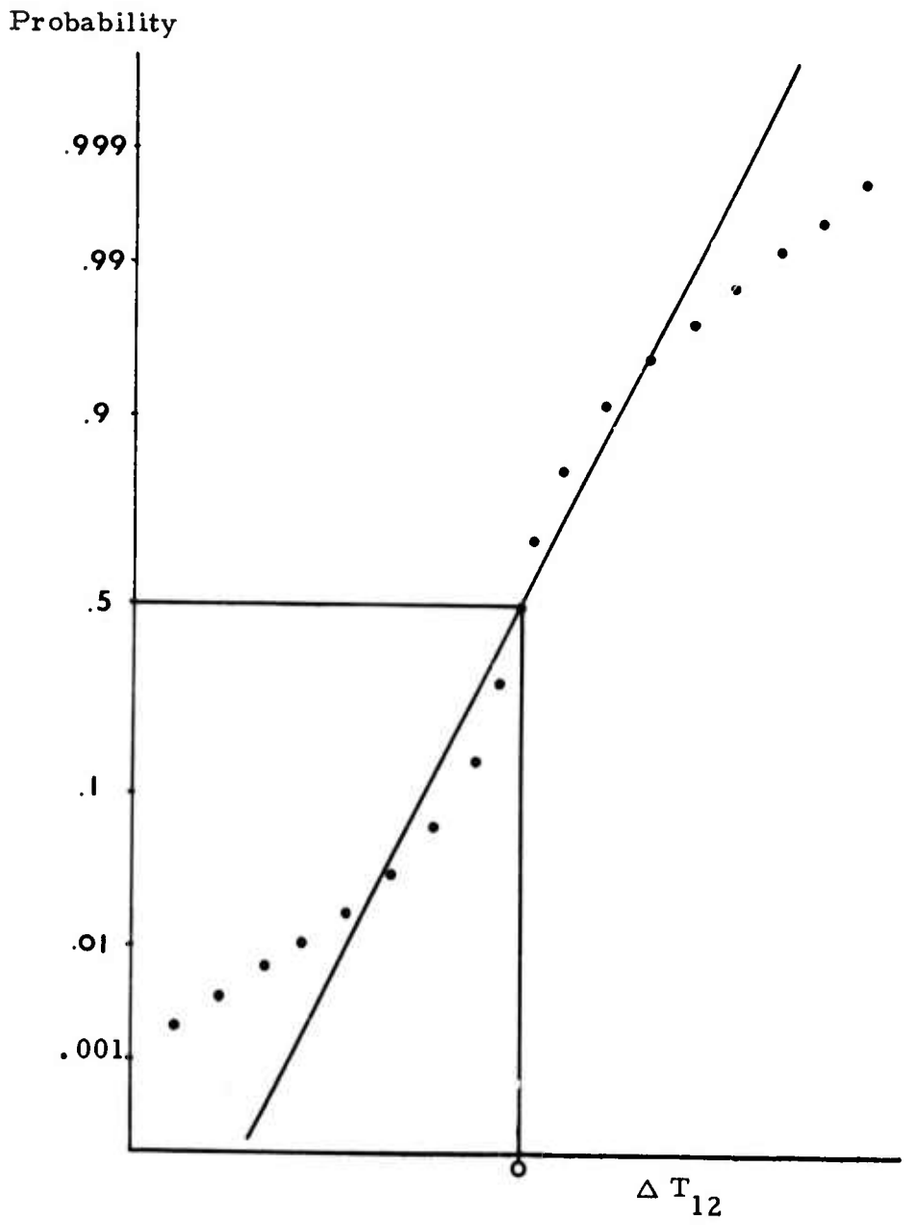

Figure 2. Cumulative probability distribution for fluctuations of Figure 1. The straight line indicates a normal distribution.

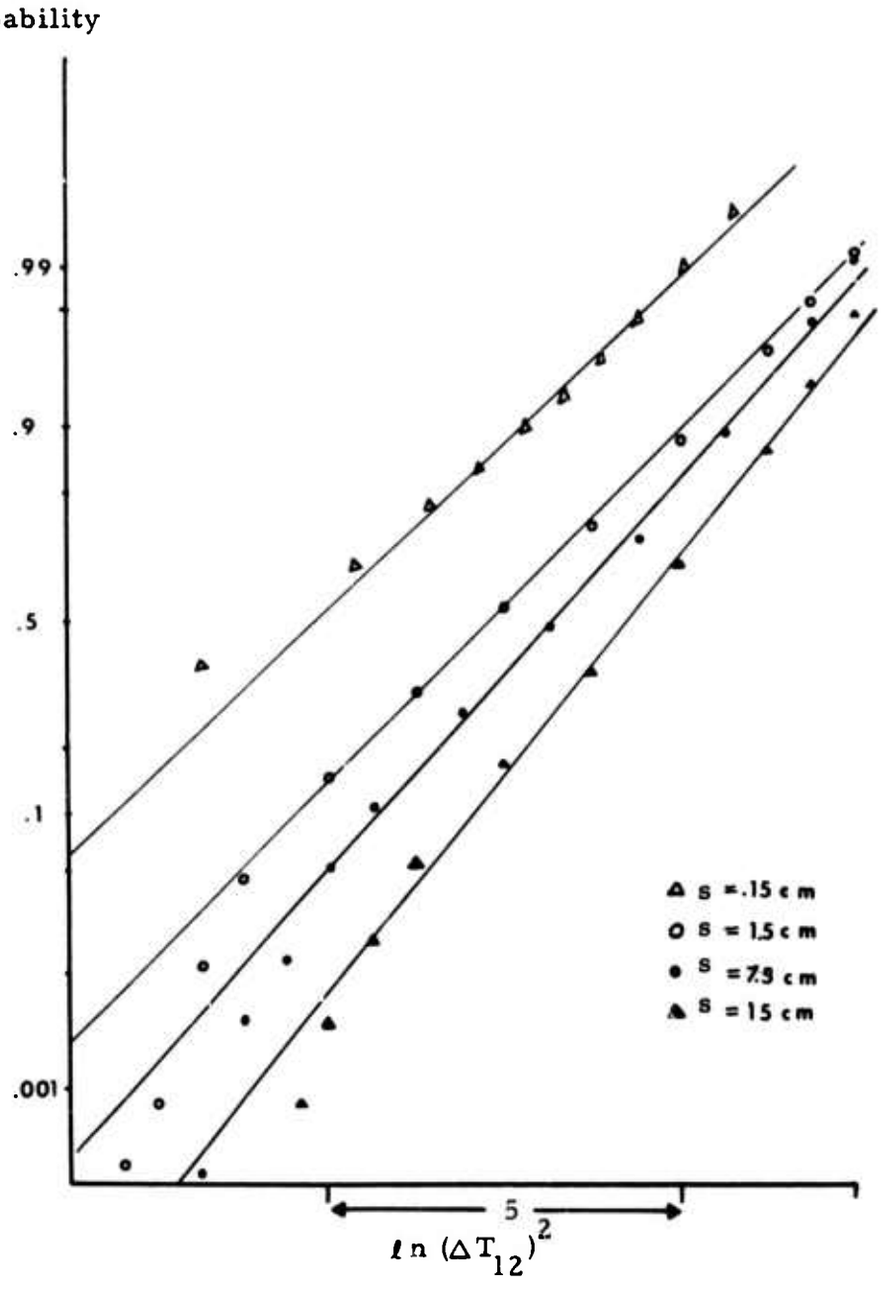

Figure 3. Cumulative probability distribution for log squared temperature-difference fluctuations, for various averaging (smoothing) scales(s). (Averaging scale = averaging time x wind speed)

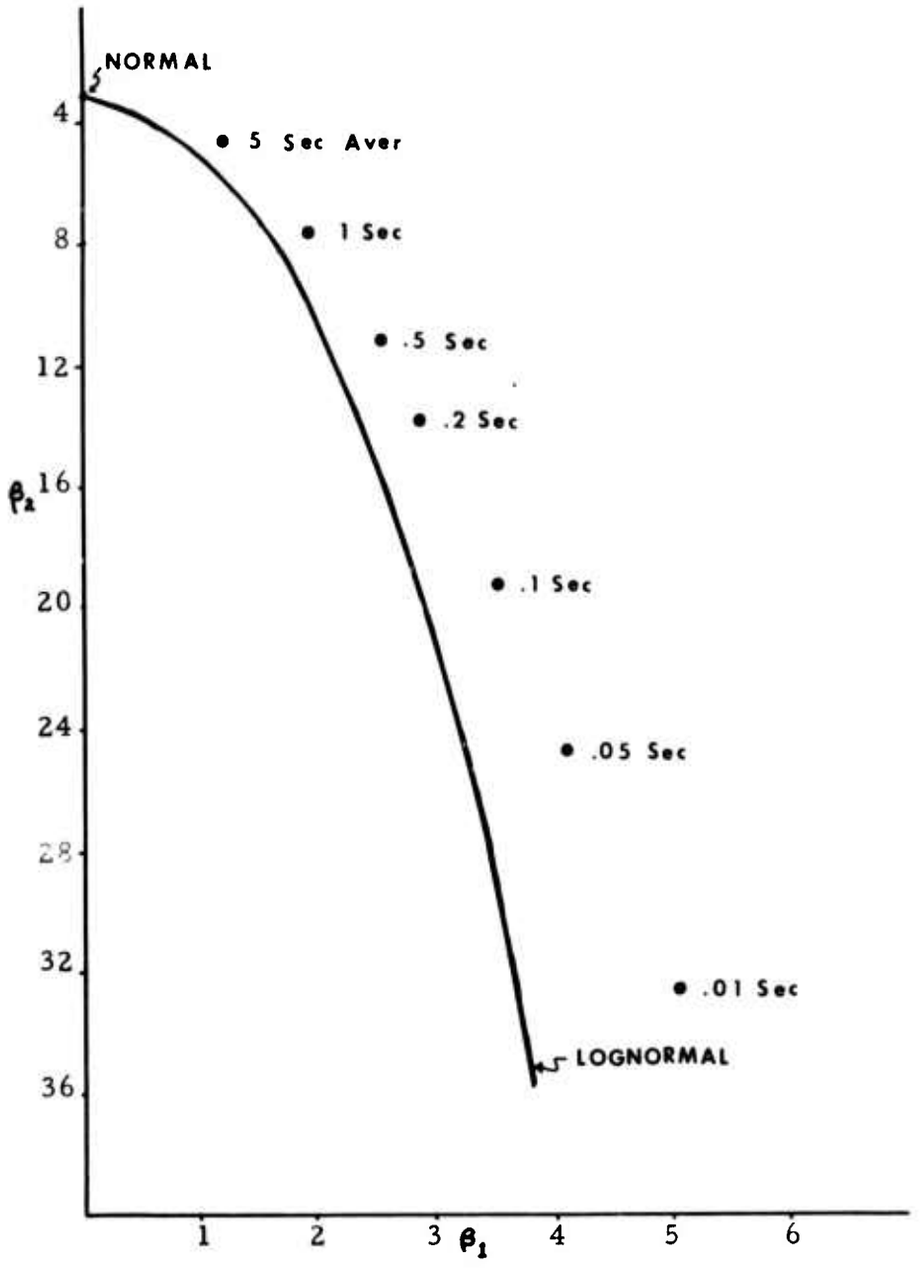

Figure 4. Beta diagram for moments of smoothed, squared fluctuations as in Figure 3, for various smoothing times. The wind speed was 1.5 m/sec.

large-flatness-factor process with suitable accuracy.[5]

In order to relate these short-term measures of mean-square temperature fluctuations to the "strength of turbulence" as utilized in propagation theory, a minimum averaging time is in fact required. Roughly speaking, this averaging time (spatial scale) must correspond to the lowest frequencies (largest scales) in the turbulence fluctuations which are of interest in the propagation phenomena. For the case of scintillations (but not necessarily for phase effects), we may designate this critical scale as the outer scale of the inertial subrange (L_o). If we average over a smaller scale, we do not obtain meaningful measures; if we average over much larger scales, we lose details of interest in the short-term problem. The mean-square temperature-difference fluctuations, for averaging times (τ) $\geq$ (L_o/v), where v is the wind speed, will be referred to in this report as the "short-term C_n^2" or $C_{n_\tau}^2$. It is apparent from Fig. 4 that the statistics of a series of measurements of $C_{n_\tau}^2$ with a given τ will be log-normal-like, and will approach normality only if τ is sufficiently long, which is not the interesting case.

We note as a side point that the integral of any stationary, ergodic process is known to be asymptotically gaussian. This is true regardless of the probability distribution of the process, and may be taken as a generalization of the Central Limit Theorem.[6]

Further statistical properties of the mean-square fluctuations will be discussed in later sections.

B. Integral Scales for Averaged Quantities

As is apparent from the preceding discussion, we will be generally concerned with random processes which are defined as short-term averaged or smoothed versions of more fundamental random processes. An important parameter for any random process is its "integral scale", which is a measure of the decorrelation time for the process. In this section, we will show that the integral scale for a smoothed process, where the averaging time is greater than the characteristic time scales of the original process, approaches (1/2) the averaging time itself. That this is so can

---

5. H. Tennekes, J. C. Wyngaard, J. Fluid Mech. 55, 93-103 (1972).
6. J. L. Lumley, "Stochastic Tools in Turbulence", Acad. Pr., 1970.

be seen intuitively by noting that smoothing corresponds to low-pass-filtering, and if the filter cut-off frequency is below the characteristic frequencies of the original process, then the lowest significant frequency (or reciprocal integral scale) in the smoothed process will be the filter cut-off frequency (Fig. 5).

To show this formally, we generalize the development of Ref. 7. We define $\rho(t')$ as the normalized autocorrelation or autocovariance function of the basic (stationary, ergodic) random process $f(t)$, and write the integral scale of f as

$$I_f = \int_o^\infty \rho(t')dt' \tag{1}$$

We then define the smoothed random process $g_\tau(t)$ as

$$g_\tau(t) = \frac{1}{\tau}\int_{-\tau/2}^{\tau/2} f(t+t'')dt'' \tag{2}$$

where the averaging time is τ. For simplicity, we assume that f,g have zero mean, and defining σ^2 as the variance of f, we write the auto-covariance of g_τ as

$$\left\langle g_\tau\,(t+t')\; g_\tau\,(t)\right\rangle = \frac{1}{\tau^2}\left\langle \int_{-\tau/2}^{\tau/2} f(t+t''+t')dt'' \int_{-\tau/2}^{\tau/2} f(t+t''')dt'''\right\rangle$$

$$= \frac{\sigma^2}{\tau^2}\int_{-\tau/2}^{\tau/2}\int_{-\tau/2}^{\tau/2} dt''dt'''\rho(t'+t''-t''')$$

$$= \frac{\sigma^2}{\tau^2}\int_{-\tau/2}^{\tau/2} dt \int_{-\tau/2-t}^{\tau/2-t} dt''\rho(t'+t'')$$

We then integrate by parts:

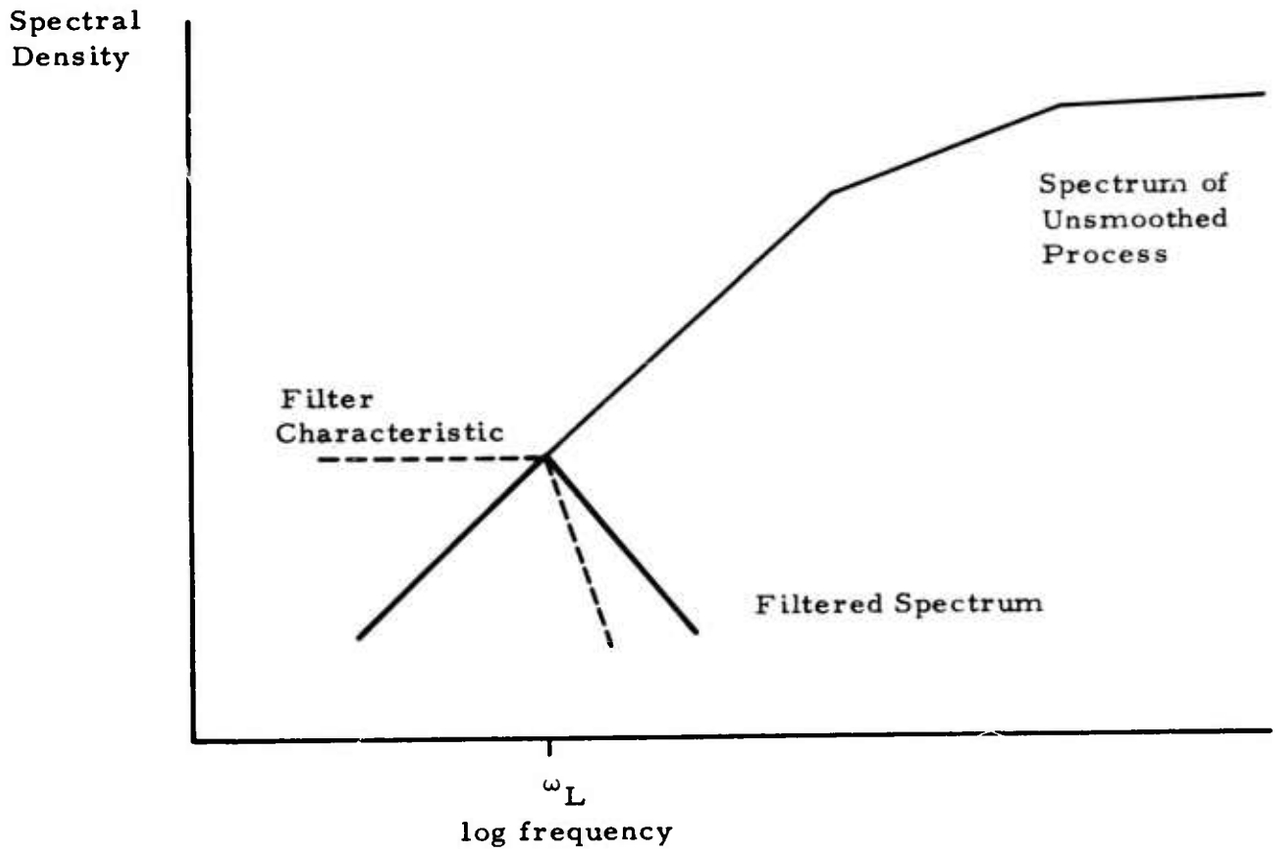

Figure 5. Illustration of the effect of low-pass filtering (smoothing) on power spectrum (and therefore integral scale) of a random process.

$$\left\langle g_\tau(t+t')\ g_\tau(t)\right\rangle = \frac{\sigma^2}{\tau^2}\left\{\left(t\int_{-\tau/2-t}^{\tau/2-t}\rho(t''+t')dt''\right)\Bigg|_{-\tau/2}^{\tau/2} - \int_{-\tau/2}^{\tau/2} t\,[\rho\,(-\tau/2-t+t') - \rho\,(\tau/2-t+t')]dt\right\}$$

$$= \frac{\sigma^2}{\tau^2}\left\{\left(\tau/2\int_{-\tau}^{o}\rho(t''+t')dt'' + \tau/2\int_{o}^{\tau}\rho(t''+t')dt''\right) - \int_{o}^{\tau}(t''-\tau/2)\rho(t'-t'')dt'' - \int_{\tau}^{o}(\tau/2-t'')\rho(t'+t'')dt''\right\}$$

$$= \frac{\sigma^2}{\tau^2}\left\{\tau/2\int_{o}^{\tau}\rho(t'-t)dt + \tau/2\int_{o}^{\tau}\rho(t'+t)dt + \int_{o}^{\tau}(\tau/2-t)\rho(t'-t)dt + \int_{o}^{\tau}(\tau/2-t)\rho(t'+t)dt\right\}$$

$$= \frac{\sigma^2}{\tau^2}\int_{o}^{\tau}(\tau-t)[\rho(t'-t) + \rho(t'+t)]dt$$

$$= \frac{\sigma^2}{\tau}\int_{o}^{\tau}(1-t/\tau)\,[\,\rho(t'+t) + \rho(t'-t)]\ dt \qquad (3)$$

As a special case we note that[7]

$$\left\langle g_\tau^2 \right\rangle = \frac{2\sigma^2}{\tau} \int_0^\tau (1-t/\tau)\rho(t)dt \tag{4}$$

Also, we integrate the autocovariance of g_τ to obtain:

$$\int_0^\infty \left\langle g_\tau(t+t')g_\tau(t) \right\rangle dt' = \frac{2\sigma^2}{\tau} I_f \int_0^\tau (1-t/\tau)dt$$

$$= \sigma^2 I_f \tag{5}$$

The integral scale of g_τ is thus given by (5) and (4) as

$$I_{g_\tau} = \frac{\sigma^2 I_f}{\left\langle g_\tau^2 \right\rangle} = \frac{I_f \ \tau}{2\int_0^\tau (1-t/\tau)\rho(t)dt} \tag{6}$$

Finally, if $I_f << \tau$, then the integral is equal to I_f, and

$$\lim \ I_{g_\tau} = \tau/2 \quad , \tag{7}$$

which is the desired result.

Typical temperature-difference fluctuations with various smoothing times (τ) are shown in Fig. 6, and the autocorrelation functions in Fig. 7. In Fig. 8, the computer integral scales are shown as a function of τ, and it is seen that Eq. (7) is verified.

The decorrelation time of the unsmoothed temperature difference fluctuations is fundamentally on the order of the (probe spacing ÷ v) and will normally be small compared to that corresponding with the outer scale.

---

7. S. A. Collins and G. W. Reinhardt, "Investigation of Laser Propagation Phenomena", RADC-TR-71-248, August 1971, Electroscience Laboratory, Ohio State University. (AD734 547)

(a)

(b)

(c)

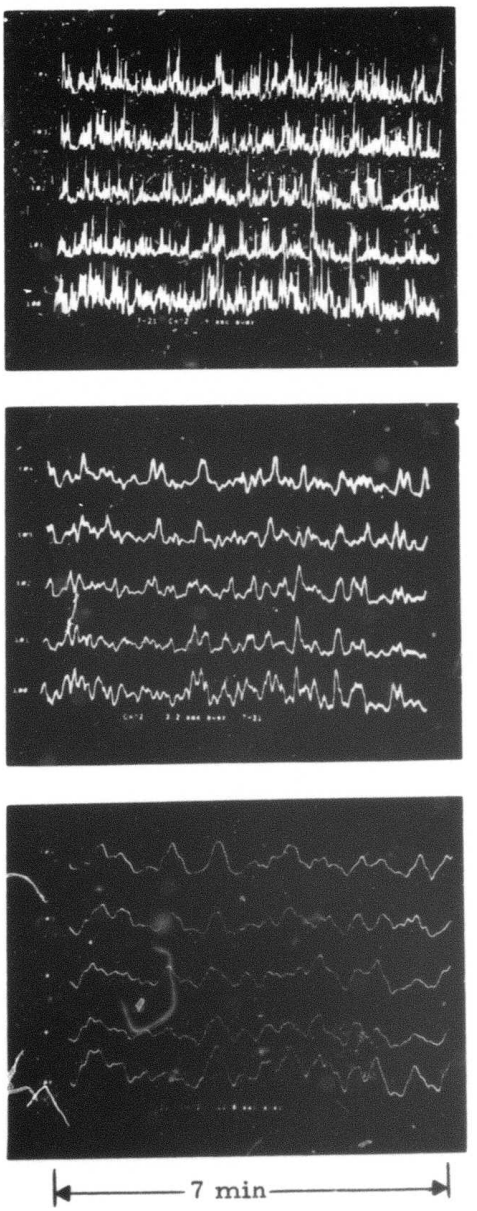

Figure 6. Squared temperature-difference fluctuations for various smoothing times (τ).

a. τ = 0.4 sec.
b. τ = 3.2 sec.
c. τ = 12.8 sec.

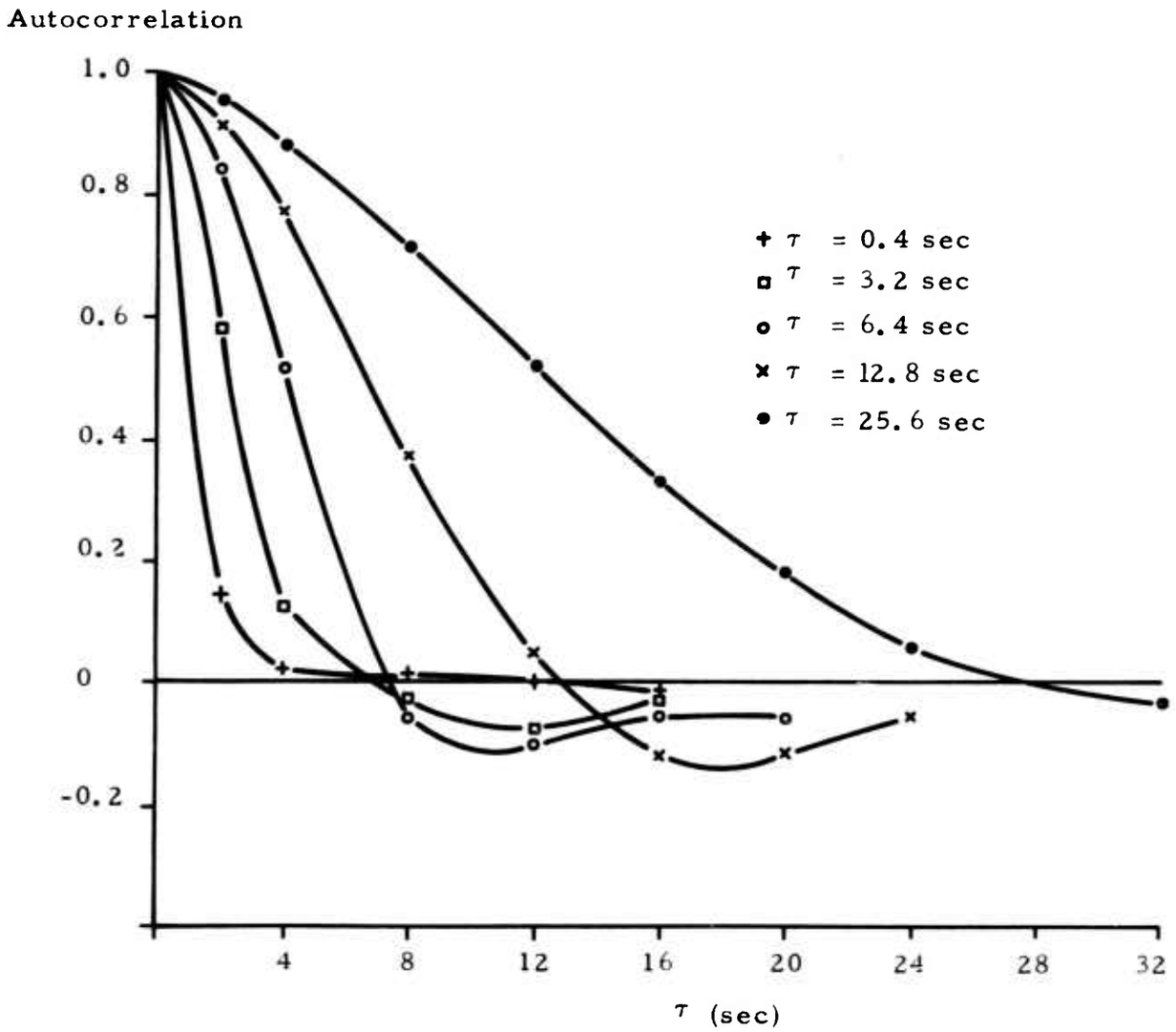

Figure 7. Autocorrelation function of smoothed fluctuations as in Figure 6, for various smoothing times.

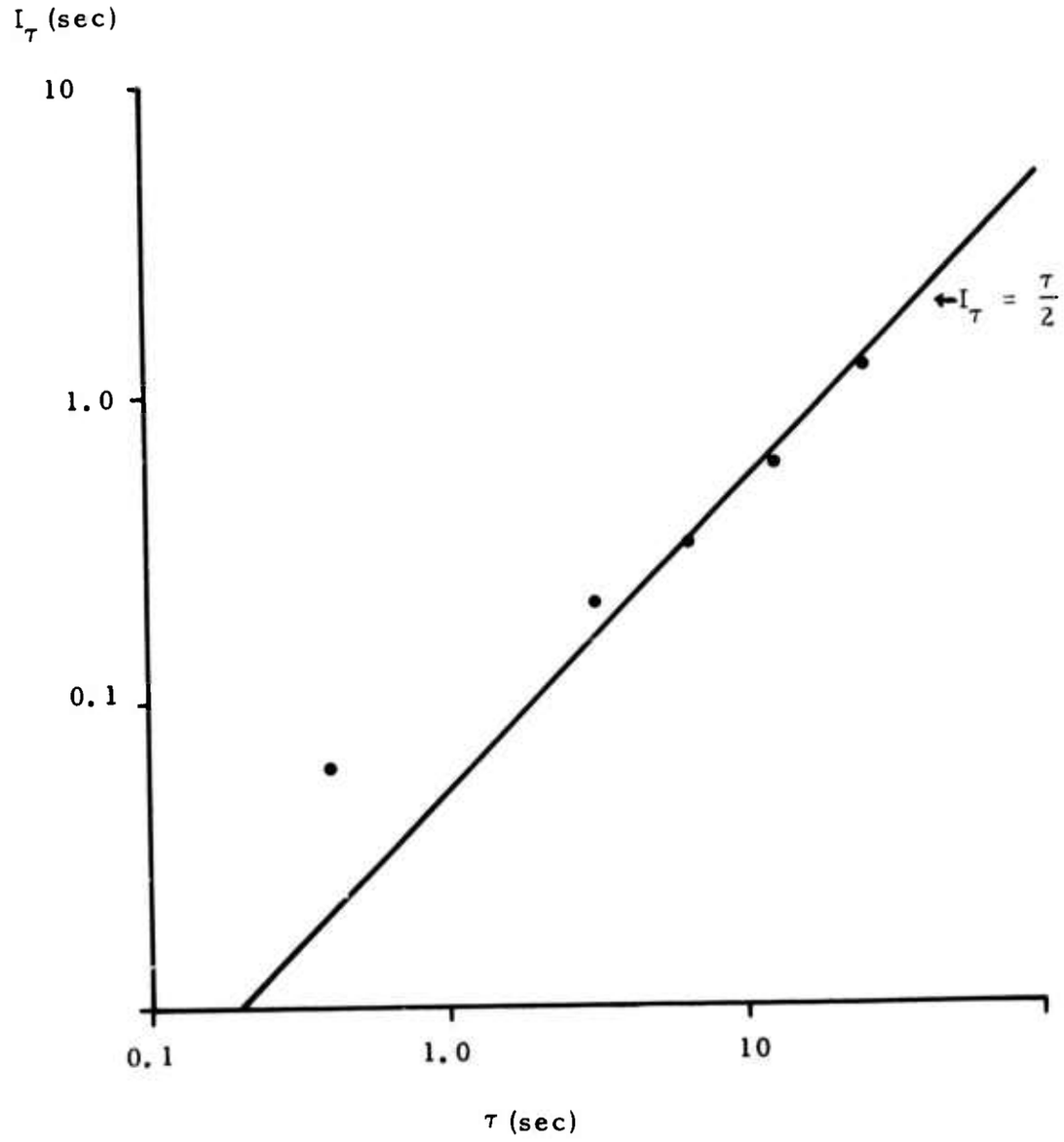

Figure 8. Computed integral scales I_τ of the smoothed processes corresponding to Figures 6 and 7, vs. smoothing time (τ).

Therefore, in practical measurements of C_n^2, the integral scale will be $\tau/2$. The same relationship between the averaging time and integral scale of a short-term average will obviously also apply to propagation quantities such as the log amplitude variance of scintillation, which tends to have an integral scale which is an order of magnitude smaller than that of the thermal fluctuations. For the data of Fig. 8, the unsmoothed microthermal scale was $\approx$ 0.6 sec., while the optical and (10 micron) infrared scales were 40 and 60 msec respectively.

C. Large-Scale Intermittency

The practical definition of an "intermittent" or "sporadic" random process is that such a process has an envelope or strength which varies much more slowly than the process itself, but changes significantly over observation times of interest. Since the concept of varying "strength" or "envelope" implies short-term averaging of the second moment, we may relate this concept to the relative time behavior of the (short-term-averaged) first and second moments.

The question of long-term stationarity of a process is often unanswerable and moot; for mathematical convenience, we assume ultimate stationarity and model the process in terms of what we learn during the limited period of observation. It is apparent that intermittency or sporadicity as defined here is not basically related to questions of stationarity.

Atmospheric turbulence, as manifested in the temperature difference fluctuations between two probes, often exhibits intermittency, e.g., in the presence of plumes, or in poorly-developed turbulence. An example is shown in Figure 9a. We are interested in applying all of the statistical considerations of this discussion to the intermittent case as well as to the simpler condition of large-scale uniformity.

The intermittent process has what at first are discerned to be peculiar properties. The slow envelope fluctuations do not represent additive low frequencies in the process, but rather, are indications of narrow sidebands around high-frequency spectral components. (Additive

low frequencies may exist in single-probe microthermal measurements, and may relate to stationarity problems, but they do not relate to the scintillation phenomena of interest here.) Since low frequencies are not present, the autocorrelation function of the process does not have a tail and does not manifest the intermittency. Hence, as will be discussed in a later section, the averaging-time considerations of Ref. 7 must be used with care in such a case.

In order to exhibit the low frequencies in the envelope, we must perform a nonlinear operation, such as taking the absolute value (Fig. 9b) or squaring. This effectively convolves the narrow sidebands around each high-frequency component, resulting in additive low frequencies. The autocorrelation function then exhibits the effects of the intermittency. As discussed in the following section, an intermittent process (z) of this type may be modelled as the product of (xy) of fast (x) and slow (y) processes, where the latter (envelope) process is always zero or positive. This model may in turn be related to the integral scales of interest.

In the simplest model for intermittent turbulence, the slow envelope process of the preceding paragraph has only two values, 0 and 1. Although this has on occasion given a reasonable fit to experimental data,[8] we find that in general it is not a good approximation. To explore this question further, we consider a typical example. In Fig. 10a we again show the fluctuations of Fig. 9, and the absolute value smoothed by means of digital RC filtering with progressively longer averaging times. The same is shown in Fig. 10b, using digital boxcar integration for smoothing. In order to avoid smearing the character of the intermittent envelope, the maximum smoothing time shown is 0.5 sec.

The probability distributions for the basic and smoothed processes of Fig. 10 are shown in Fig. 11. The distribution function for the envelope, with 0.5 sec smoothing, is seen to have a slight tendency for a double-humped appearance, but is poorly approximated by a two-level function.

---

8. R. S. Lawrence, G. R. Ochs, S. F. Clifford, J. Opt. Soc. Am. 60, 826 (1970).

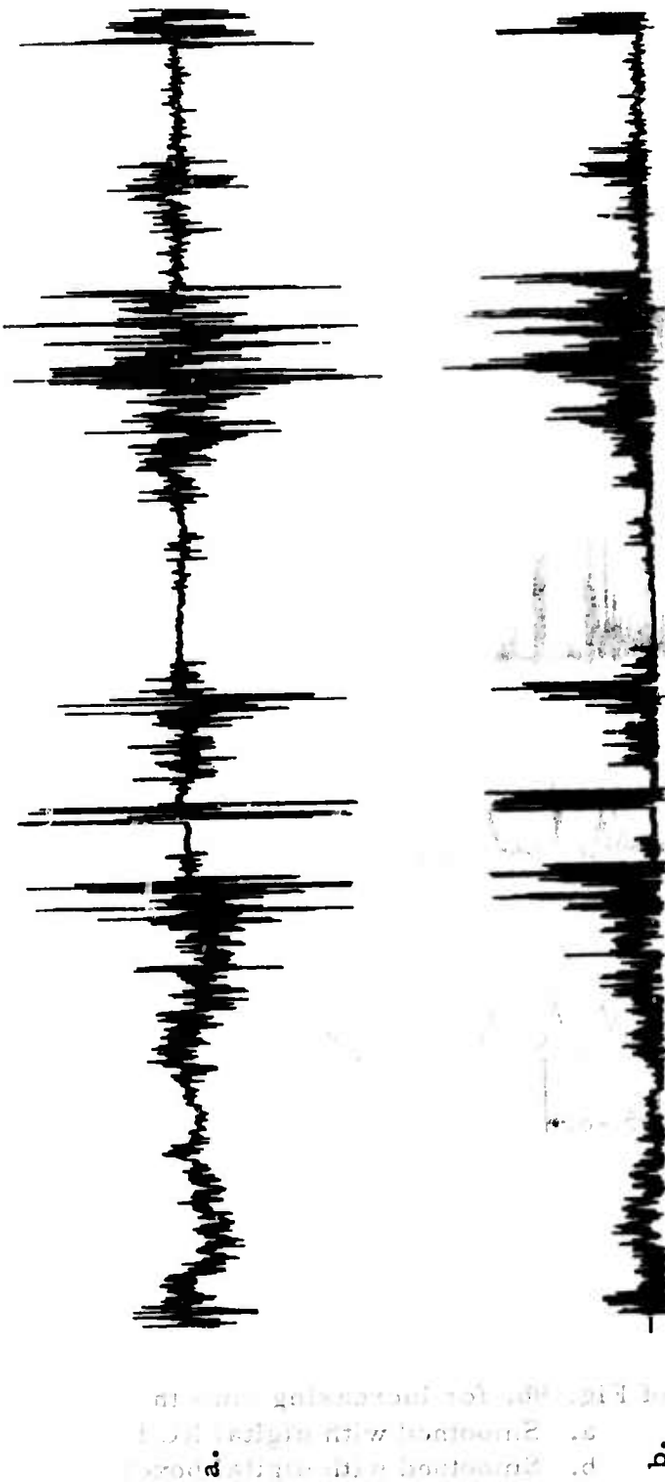

Figure 9. Intermittent temperature-difference fluctuations.

a. $\Delta T_{12}(t)$

b. $|\Delta T_{12}(t)|$

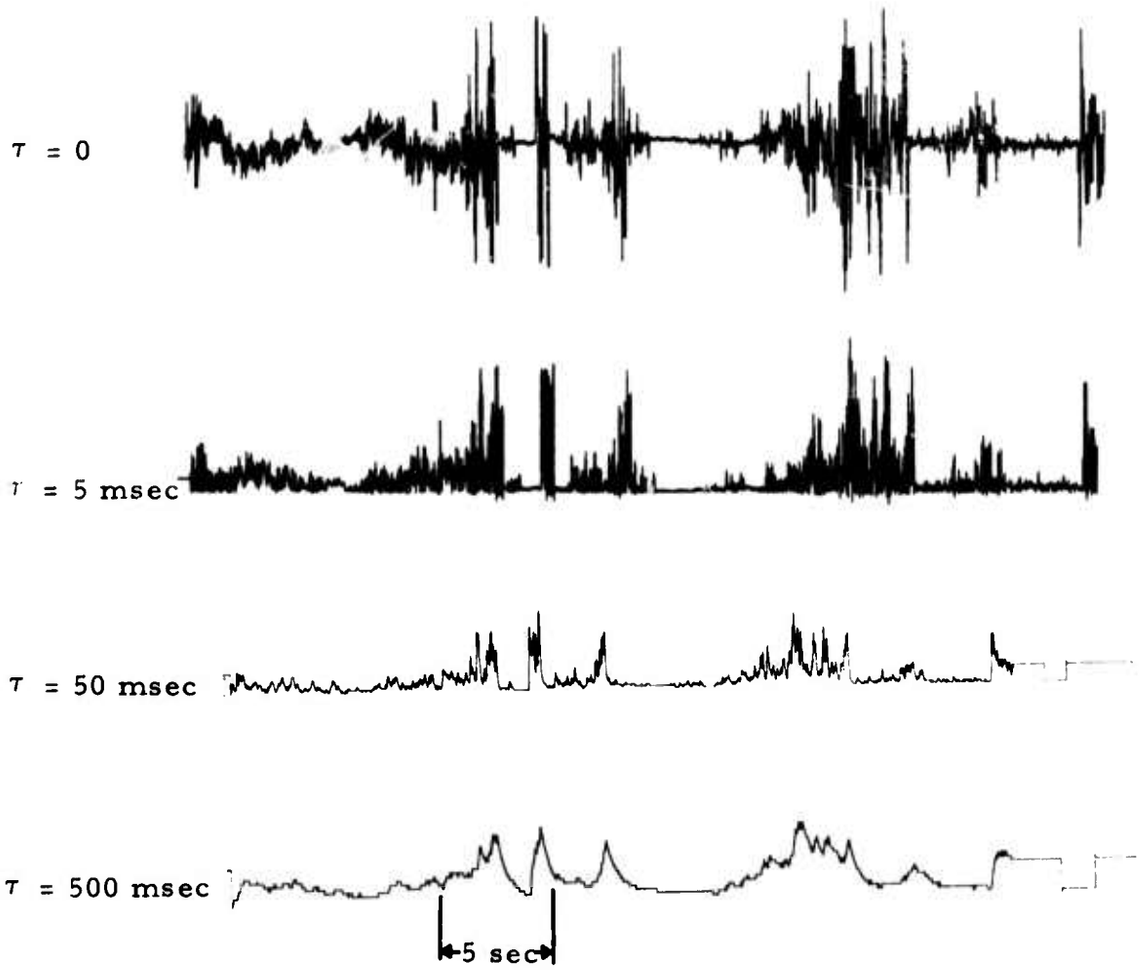

Figure 10a. Fluctuations of Fig. 9b. for increasing smoothing times (τ).
a. Smoothed with digital RC filter.
b. Smoothed with digital boxcar integrator.

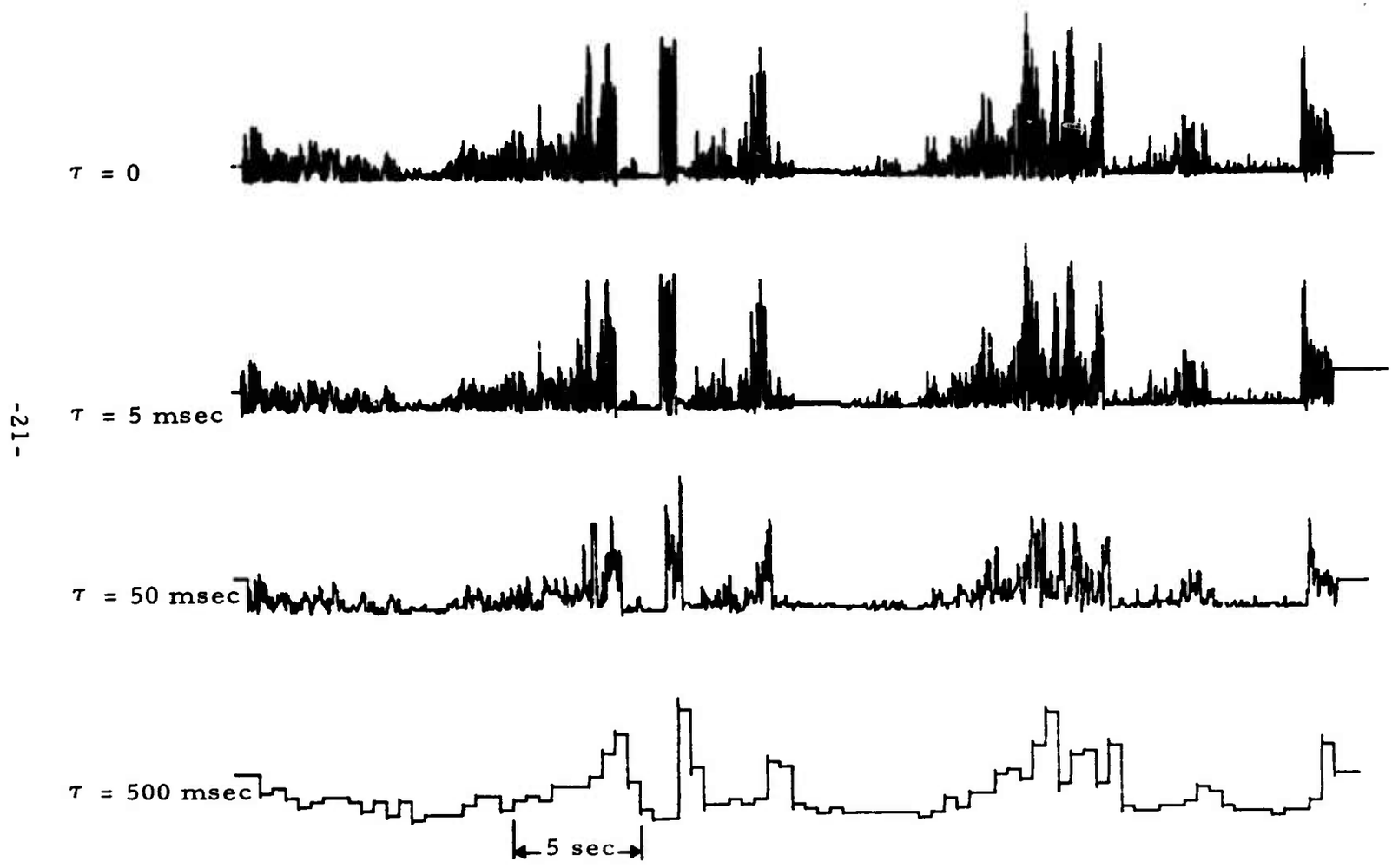

Figure 10b.

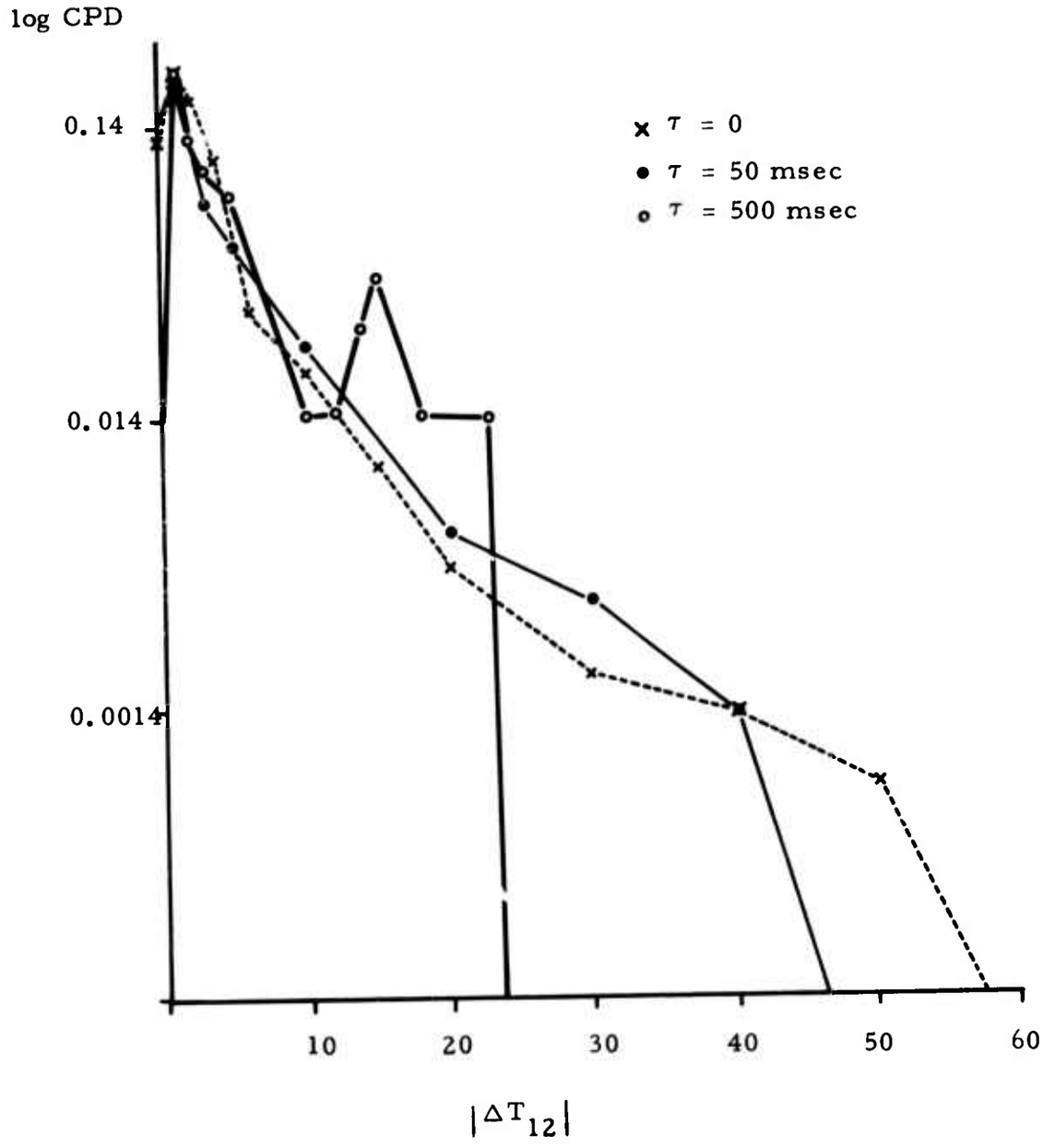

Figure 11. Cumulative probability distribution (CPD) for smoothed fluctuations of Fig. 10, for various smoothing times (τ).

If we again consider the multiplicative model, we postulate that the fast process (x) has the high-flatness-factor statistics of the fundamental, unsmoothed microthermal process of Sec. II-A. The envelope distribution (y) will be maximum at small values and will have a distribution like that (0.5 sec) in Fig. 11. The probability distribution (P_z) of the composite process ($z = xy$) may be written as[9]

$$P_z dz = \int_0^\infty P_x(z/y)\ P_y(y)\ 1/y\ dy\ dz \qquad (8)$$

We therefore expect the composite intermittent process to have a probability distribution with a fairly high flatness factor but, owing to the envelope distribution, it will have more smearing or less of a log-normal-like character than in the non-intermittent case.

Although we do not yet have a sufficiently long data record of intermittent fluctuations to generate a beta diagram vs. smoothing time for squared fluctuations, such as that of Fig. 4 for the non-intermittent case, we can speculate on the results of such a plot. The unsmoothed fluctuations will have a smaller flatness factor than in the non-intermittent case. For intermediate smoothing times (such as 0.5 sec in Fig. 10), which exhibit the intermittent envelope, the same will be true. However, as discussed in the following section, the low frequencies relating to intermittency will cause the integral scale of these squared fluctuations to be larger than in the non-intermittent case, and hence the approach to a normal distribution with increased smoothing times will be more gradual. These comparisons of course assume an identical wind-speed normalizing factor.

We note that the meteorological and fluid mechanical literature contains many discussions of microscale intermittency and, in some cases, its relationship to large-scale intermittency. Many of these have been referenced in earlier reports on this program. The field is clearly in a state of flux, and there is much room for more fundamental work. Our approach to macroscale intermittency is a pragmatic one, in that it avoids esoteric

---

9. G. J. Hahn and S. S. Shapiro, Statistical Models in Engineering, Wiley & Sons, 1967.

questions of generalized stationarity, the inadequacies of the energy-cascade model, etc.[10] A basic complication is that the behavior of intermittent microthermal envelopes cannot be expected to be universal but rather, will be a complicated function of meteorological and local geographical factors. Similarly, the localized regions of stronger or weaker turbulence may not be expected to be isotropic.

Contrary to some statements in the literature, it now seems clear that intermittency plays no fundamental role in such propagation phenomena as the saturation of scintillations or the generation of log normal scintillation statistics. We may therefore view the role of intermittency as simply a mechanism which increases the fluctuations in short-term-averaged propagation measurements or channel performance, and this can be quantitatively described in terms of relevant measures such as spatial envelope correlations and integral scales. These factors will be discussed further in following sections.

D. Further Discussion of Integral Scales

In a previous section we have shown that the integral scale of any smoothed process approaches one-half the averaging time as the latter increases. We have also pointed out that a slowly varying envelope or strength of a process does not have an effect on the autocorrelation, low-frequency content, or integral scale of that process. However, once we take the absolute value (rectify) or square the process, the low envelope frequencies will be directly manifested. An example of the enhanced low frequencies in the absolute value of intermittent microthermal fluctuations is shown in Fig. 12.

As a prelude to the next section, in which averaging time effects in the presence of intermittency are discussed, we show here analytically how the integral scale of an intermittent process is affected by squaring. We again model the process as the product of a fast process (x) and slow envelope process (y). Since these processes are independent, and x has zero mean, the composite process $z = xy$ also has zero mean.

---

10. Benoit Mandelbrot, "Intermittent Turbulence in Self Similar Cascades", J. Fluid Mechanics, 62, Part II, 331-358 (1974).

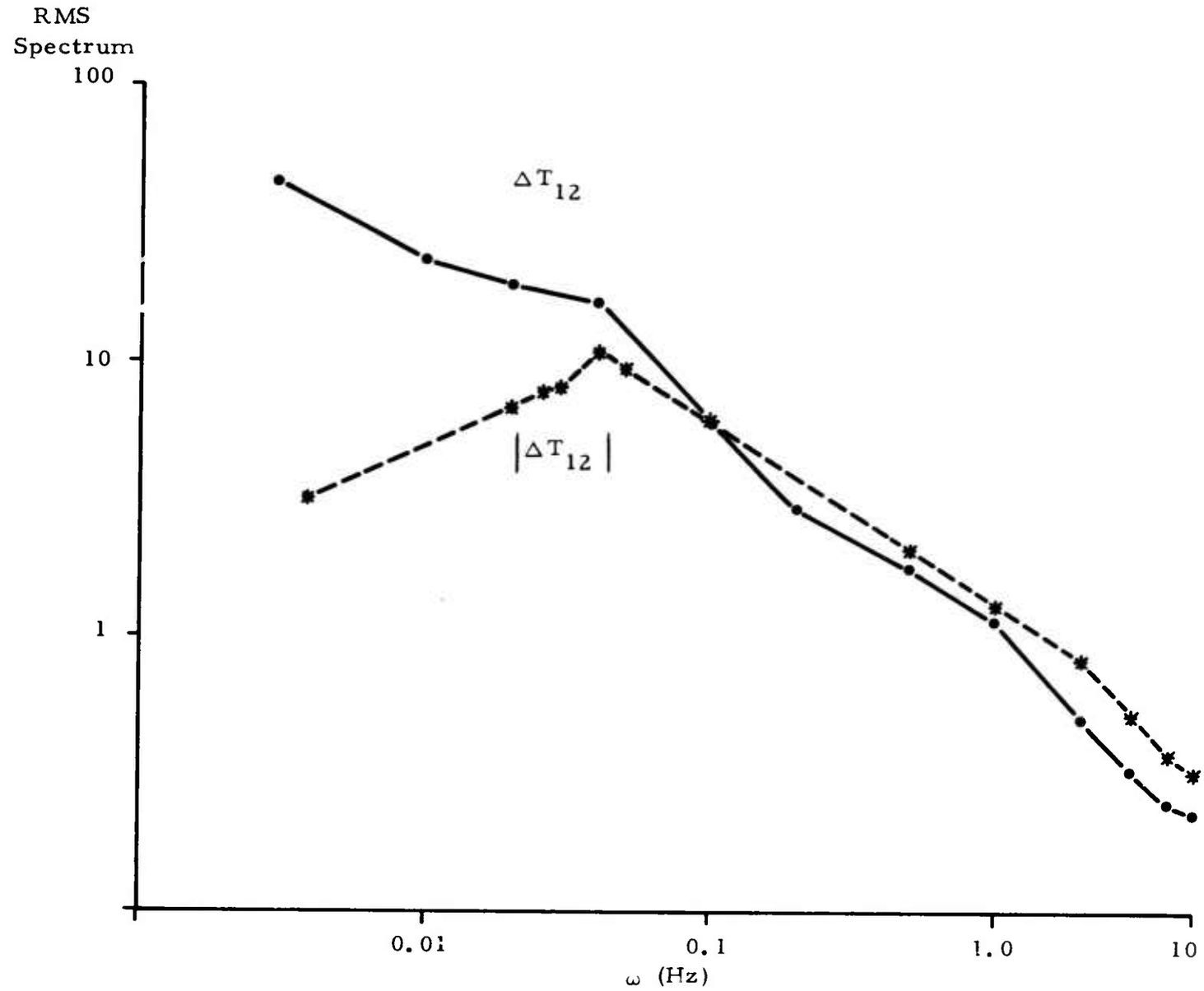

Figure 12. Comparison of power spectrum of temperature-difference fluctuations ΔT_{12} vs. that for $|\Delta T_{12}|$.

To find the integral scale of z, we write

$$I_z = \frac{\int_0^\infty \langle x(t+t')x(t)y(t+t')y(t)\rangle \, dt'}{\langle x^2\rangle \langle y^2\rangle}$$

$$\cong \frac{\langle y^2\rangle \int_0^\infty \langle x(t+t')x(t)\rangle \, dt'}{\langle x^2\rangle \langle y^2\rangle} \qquad (9)$$

$$= I_x$$

as expected. This does not manifest the intermittency.

For the integral scale of the fluctuations of z^2, we have

$$I_{z^2} = \frac{\int_0^\infty \left\{ \langle x^2(t+t')x^2(t)y^2(t+t')y^2(t)\rangle - \langle x^2\rangle^2 \langle y^2\rangle^2 \right\} dt'}{\left[\langle x^4\rangle \langle y^4\rangle - \langle x^2\rangle^2 \langle y^2\rangle^2 \right]} \qquad (10a)$$

Noting that x and y are independent, we have

$$I_{x^2} = \frac{\int_0^\infty \left\{ \langle y^2(t+t')y^2(t)\rangle \langle x^2(t+t')x^2(t)\rangle - \langle x^2\rangle^2 \langle y^2\rangle^2 \right\} dt'}{\left[\langle x^4\rangle \langle y^4\rangle - \langle x^2\rangle^2 \langle y^2\rangle^2 \right]} \qquad (10b)$$

We expand this to write

$$I_{z^2} = \frac{\int_0^\infty \left\{ \langle y^2(t+t')y^2(t)\rangle \langle x^2(t+t')x^2(t) - \langle x^2\rangle^2 \rangle \right\} dt'}{\left[\langle x^4\rangle \langle y^4\rangle - \langle x^2\rangle^2 \langle y^2\rangle^2 \right]}$$

$$+ \frac{\int_0^\infty \left\{ \langle x^2 \rangle^2 \left\langle y^2(t+t')y^2(t) - \langle y^2 \rangle^2 \right\rangle \right\} dt'}{\left[\langle x^4 \rangle \langle y^4 \rangle - \langle x^2 \rangle^2 \langle y^2 \rangle^2 \right]} \qquad (11)$$

$$\equiv I_{z_1}^2 + I_{z_2}^2 \quad .$$

Let us now denote the integral scales for the fluctuations of x^2 and y^2 about their means as I_x^2 and I_y^2 respectively. I_x^2 will be on the order of I_x, while I_y^2 will be much greater since y is slowly varying. Consider the first term of Eq. (11). The first or y-expectation will be $\langle y^4 \rangle$ for all t' such that the second or x-expectation is nonzero. We thus have

$$I_{z_1}^2 = \frac{\langle y^4 \rangle \cdot I_x^2 \left(\langle x^4 \rangle - \langle x^2 \rangle^2 \right)}{\langle x^4 \rangle \langle y^4 \rangle - \langle x^2 \rangle^2 \langle y^2 \rangle^2}$$

$$= I_x^2 \left[1 - \left(\frac{\frac{\langle y^4 \rangle}{\langle y^2 \rangle^2} - 1}{\beta_{2_x} \frac{\langle y^4 \rangle}{\langle y^2 \rangle^2} - 1} \right) \right]$$

$$\equiv I_x^2 (1 - \alpha), \qquad (12a)$$

where β_{2_x} is the flatness factor defined previously.* For the second term of Eq. (11), we have

---

*The term $\langle y^4 \rangle / \langle y^2 \rangle^2$ is not identical to β_{2_y}, since $\langle y \rangle \neq 0$. It may be taken as a measure of intermittency.

$$I_{z_2}^2 = \frac{\langle x^2\rangle^2 \cdot I_y^2 \left(\langle y^4\rangle - \langle y^2\rangle^2 \right)}{\langle x^4\rangle \langle y^4\rangle - \langle x^2\rangle^2 \langle y^2\rangle^2}$$

$$= I_y^2 \left[\frac{\frac{\langle y^4\rangle}{\langle y^2\rangle^2} - 1}{\beta_{2_x} \frac{\langle y^4\rangle}{\langle y^2\rangle^2} - 1} \right]$$

$$= \alpha I_y^2. \qquad (12b)$$

To examine the behavior of these expressions, we note that $\beta_{2_x} >> 1$, while $\langle y^4\rangle / \langle y^2\rangle^2 = 1$ for no intermittency and is greater in the presence of intermittency. Hence for no intermittency, $\alpha = 0$ and $I_{z_2}^2 = I_{z_1}^2 = I_x^2$ as expected. As $\frac{\langle y^4\rangle}{\langle y^2\rangle^2}$ grows, $I_{z_1}^2$ becomes somewhat less than I_x^2, while $I_{z_2}^2$ grows to a maximum of I_y^2/β_{2_x}. Hence the integral scale or decorrelation time of an unsmoothed intermittent process when squared will exhibit the long integral scale of the envelope, diminished by the high flatness factor of the basic process. This will be pertinent in the considerations of later sections.

Finally, we point out that the behavior of the integral scale when a random process is squared can serve as a quantitative indication of the degree of "intermittency" of the process; $\frac{I_{z_2}^2}{I_z}$ depends on both the envelope distribution (α) and on the envelope scale (I_y^2).

E. Averaging Time vs. Data Spread for Intermittent Turbulence

Considerations of averaging time effects on measurements of random processes have been reviewed in Ref. 7. At first appearance, there has been a paradox in the application of these results to intermittent processes, in that data-spread is expressed in terms of the integral scale (or power spectrum) of the process, while the envelope-intermittency does not show

up in these quantities. Yet, it is physically clear that intermittency can strongly affect the spread in measurements of short-term-average quantities, even though the process is truly stationary in the long term. The purpose of this section is to resolve this seeming inconsistency, and to remark on the interpretation of the results for this case.

Let us consider the stationary, intermittent process $z(t)$. We denote any sample measurement of $z^n(t)$ over an averaging time τ by $\overline{z^n}_\tau$. The integral scale of the fluctuations of z^n is again denoted by I_{z^n}, and we assume that any such integral scale is short relative to averaging times of interest.

If we now define $f(t)$ in Ref. 7 as $z(t)$, and recall that $\langle z \rangle = 0$, a simple statement of the results of Eq. (8) of that reference is that

$$\frac{\left\langle \overline{z_\tau^2} \right\rangle}{\left\langle z^2 \right\rangle} = \frac{2 I_z}{\tau} \quad . \tag{13}$$

This is not a very interesting result, because the simple deviation of sample averages of $z(t)$ from its true mean of zero is not interesting. The dependence on I_z, which does not manifest the intermittency, is clearly appropriate in the case of this measurement.

We now redefine $f(t)$ of Ref. 7 as $z^2(t)$. We then have the result that

$$\frac{\left\langle \left(\overline{z_\tau^2} - \left\langle z^2 \right\rangle \right)^2 \right\rangle}{\left\langle z^4 \right\rangle - \left\langle z^2 \right\rangle^2} = \frac{2 I_{z^2}}{\tau}$$

and[5]

$$\frac{\mathrm{Var}\ \overline{z^2}_\tau}{\left\langle z^2 \right\rangle^2} = \frac{2 I_{z^2}}{\tau} \times \frac{\mathrm{Var}\ z^2}{\left\langle z^2 \right\rangle^2} \quad . \tag{14}$$

This is the result of interest, and as discussed in the previous section, I_z^2 does manifest the intermittent envelope. To apply this result, we must know the long-term or approximate-ensemble values involved. For an intermittent process with slow envelope variations (large I_z^2), this may require a very long time. Also, the ensemble quantity $\langle \overline{z_\tau^2} \rangle$ does not apply to a limited set of measurements, and in the presence of slow intermittency, may likewise require many samples to determine approximately. However, there is no formal inconsistency.

We point out that the self-consistent averaging-time argument in Ref. 7 implicitly assumes that no long-term variations in the envelope of z(t) occur. I.e., within a time span shorter than the long-term fluctuations in the envelope fluctuations, whose existence might not even be known to the experimenter, the ensemble quantities are an abstraction; there is no way to know their true values.

We also point out that the condition that τ is much greater than the relevant integral scale is much more severe for Eq. (14) than for (13). However, shorter averaging times (e.g. corresponding to the outer scale of turbulence) may retain more information and therefore be of interest. Hence, in the presence of intermittency, the averaging time may not contain many decorrelation times for the envelope. An appropriate generalization of the above results, not requiring $\tau >> I$, may be written from Ref. 7:

$$\frac{\left\langle \left(\overline{z_\tau^2} - \langle z^2 \rangle \right)^2 \right\rangle}{\langle z^4 \rangle - \langle z^2 \rangle^2} = \frac{2}{\tau} \left[\int_0^\tau (1 - t/\tau)\, \rho_{z^2}(t)\, dt \right] , \qquad (14a)$$

where ρ_{z^2} is the autocorrelation of z^2. In the limit $\tau << I_z^2$, this equals $\rho_{z^2}(0)$, which will be much larger than the $I_z^2 << \tau$ result of Eq. (14).

F. Fourier-Stieljes Representation for Intermittent Turbulence

As mentioned above, our operational description of intermittency circumvents the need for the complications of generalized stochastic theory.[6, 10, 11, 12] Although it was not originally obvious, it may be easily shown that intermittency, as modelled here, does not introduce difficulties in the conventional spectral representation for a random process. This may be shown as follows.

The conventional Fourier-Stieljes spectral representation for a stationary random process f(t) is given by

$$f(t) = \int_{-\infty}^{\infty} e^{i\omega t} dF(\omega) \quad ,$$

where $dF(\omega)$ is a random function of the increment in ω. More explicitly,

$$\int_{-\infty}^{\infty} e^{i\omega t} dF(\omega) \equiv \lim_{\Omega \to \infty} \int_{-\Omega}^{\Omega} e^{i\omega t} dF(\omega)$$

and

$$\int_{-\Omega}^{\Omega} e^{i\omega t} dF(\omega) \equiv \lim_{||\Delta\omega_k|| \to 0} \sum_{k=1}^{N} e^{i\omega_k' t} \left[F(\omega_k) - F(\omega_{k-1}) \right] \qquad (15)$$

where

$$-\Omega \equiv \omega_0 < \omega_1 < \omega_2 \cdots\cdots < \omega_N \equiv \Omega$$

$$\omega_k > \omega_k' > \omega_{k-1}$$

$$||\Delta\omega_k|| \equiv \max \; |\omega_k - \omega_{k-1}|$$

Since the autocorrelation of f(t) cannot depend on t, the random variables $F(\omega)$ and $F(\omega_{k-1})$ must be uncorrelated for $\omega_k \neq \omega_{k-1}$. This follows from

---

11. A. M. Yaglom, An Introduction to the Theory of Stationary Random Functions, Prentice-Hall, Inc., 1962.
12. J.L.Doob, Stochastic Processes, Wiley & Sons, 1953.

writing the autocorrelation as

$$\left\langle f(t)f^*(t+t')\right\rangle = \left\langle \int_{-\infty}^{\infty} e^{i\omega t} dF(\omega) \int_{-\infty}^{\infty} e^{-i\omega'(t+t')} dF(\omega') \right\rangle$$

$$= \int_{-\infty}^{\infty} e^{-i\omega' t'} e^{it(\omega-\omega')} \left\langle dF(\omega) dF(\omega')\right\rangle \quad . \tag{16}$$

Hence, we have the familiar requirement that the spectrum of a (wide-sense) stationary process have "orthogonal increments":

$$\left\langle dF(\omega) dF(\omega')\right\rangle = \delta(\omega-\omega')\left\langle |dF(\omega)|^2\right\rangle \quad . \tag{17}$$

Now consider the multiplicative model of an intermittent process, $z = xy$. Since $x(t)$ and $y(t)$ are independent stationary processes, the autocorrelation of $z(t)$ may be written as

$$\begin{aligned} \left\langle z(t)z(t+t')\right\rangle &= \left\langle x(t)x(t+t')\right\rangle \left\langle y(t)y(t+t')\right\rangle \\ &\equiv \rho_x(t')\rho_y(t') \\ &\equiv \rho_z(t') \end{aligned} \quad . \tag{18}$$

Hence $z(t)$ is trivially shown to be stationary, with a spectrum which also has orthogonal increments.

The key to this result is, of course, the independence of the fast fluctuations and the modulating envelope. If they are stationary but not independent, the probability distribution of the product (Eq. 8) involves a conditional probability which in turn involves the joint distribution of x and y. It is known that the latter may not be stationary in such a case,[13] so that $z = xy$ may not be stationary.

---

13. A. Papoulis, Probability Random Variables and Stochastic Processes, McGraw-Hill, 1965.

Most of our remarks here involve double-probe (or high-passed) microthermal data appropriate to scintillations, in which independence of the envelope and basic fluctuations is probably a valid assumption. However, in the case of single-probe data, which relates to optical/infrared phase fluctuations and which has additive low frequencies, this independence is clearly violated, e.g., in the case of plumes of warmer, more turbulent air relative to the surroundings.

We intend to subject the hypothesis of orthogonal increments to computer testing, for single and double-probe fluctuations exhibiting intermittency.

G. Spatial Correlations of the Microthermal Envelope

As will be seen in a later section, the most important property of the spatial microthermal envelope is its two-point correlation function down the propagation path. This determines the number of independent "cells" traversed by the path, and consequently the fluctuation in the short-term strength of scintillations. Since measurements of the microthermal field per se are normally made with instrumentation at one or more points, where the wind transports the turbulence structure past each probe, we are also interested in the "frozen-in" or Taylor hypothesis philosophy as it applies to the envelope. Similarly, since the wind direction is in general randomly related to the path vector, we are interested in the horizontal isotropy of the envelope.

These considerations of isotropy and taylor hypothesis as applied to the microthermal envelope are quite different from those for the basic fluctuations themselves. The term "envelope" implies some degree of time or spatial averaging, and the temporal-spatial scales involved are larger than the outer scale (L_o). Hence fundamental similarity arguments are not applicable, and universal behavior can hardly be expected.

Consider the microthermal sensor configuration of Fig. 13a, where each point represents a two-meter high differential probe pair, for which the output is squared and short-term-averaged. This squared, smoothed output is then cross-correlated with that from each other point, as a function of time lag. When little or no smoothing is used, and the point

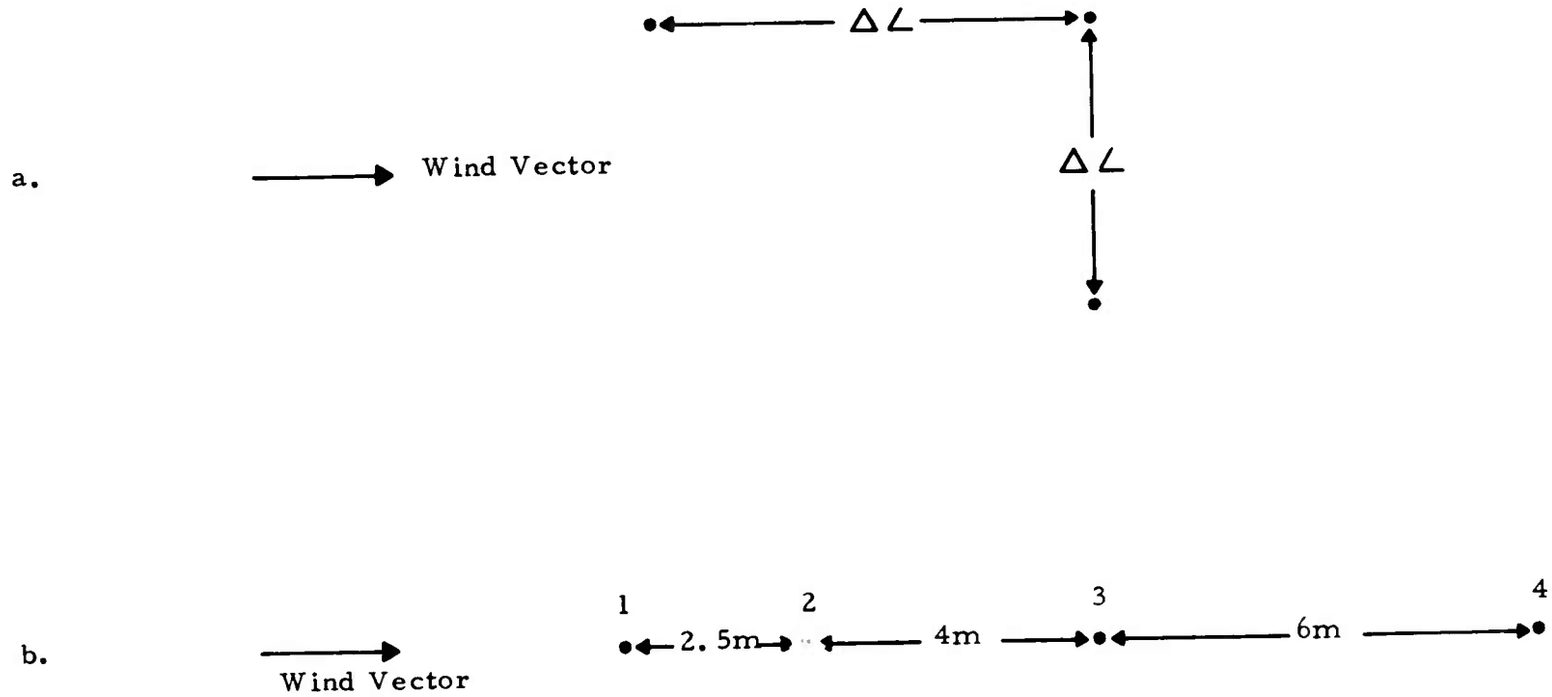

Figure 13. Deployment of microthermal measurement systems. Each point represents a probe-pair (for temperature-difference measurements).
a. Two-dimensional array
b. One-dimensional array.

separations (ΔL) in each direction are 1.5 m, the normalized cross correlation for adjacent points (12 or 23) is typically 0.3 at zero time lag; it falls monotonically for points 23 perpendicular to the wind, while for points 12 along the wind, it has the same zero-lag value and exhibits a secondary peak of typically 0.1 at a time lag corresponding roughly to the "Taylor interval" (separation divided by wind speed). However, if the point separation is increased to 2.5 m, the zero-lag correlation is very small (0.02) and independence is exhibited at all time lags. Hence, for the squared but unsmoothed case, where the additive low envelope frequencies are dominated by the high frequencies, a complete breakdown in correlation is seen for separations on the order of the outer scale. Inside this scale, very good isotropy and significant frozen-in structure are observed.

Now consider the envelope correlations with significant averaging time. Just as the averaging time affects and can determine the integral scale for an autocorrelation function, it may also be expected to affect the isotropy and frozen-in character of the spatial envelope. Consider the probe-pair measurement points, 2 meters high and separated as in Figure 13b (eight probes total). This arrangement provides point separations of 2.5, 4, 6, 6.5, 10, and 12.5 m. Using 0.4 sec averaging with a 3.5 m/sec wind along the line joining the points, the respective mean-square fluctuations were as shown in Fig. 14. The Taylor time lag and decaying correlation are qualitatively evident. Note that the averaging time corresponds spatially to a scale (1.4 m) on the order of L_o.

The time-lagged, spatial correlation functions are shown for shorter separations in Fig. 15a and for larger separations in Fig. 15b. The spatial and temporal autocorrelation functions are shown in Fig. 16, showing a breakdown in agreement at approximately 8 m. Clearly, smoothing increases the realm of frozen-in envelope behavior substantially, by emphasizing the low frequencies in the envelope. The spatial vector-correlation effects (isotropy) of averaging will be considered further in the next section. The details, of course, will depend on the behavior of the (two-dimensional) spatial frequencies below that determined by the

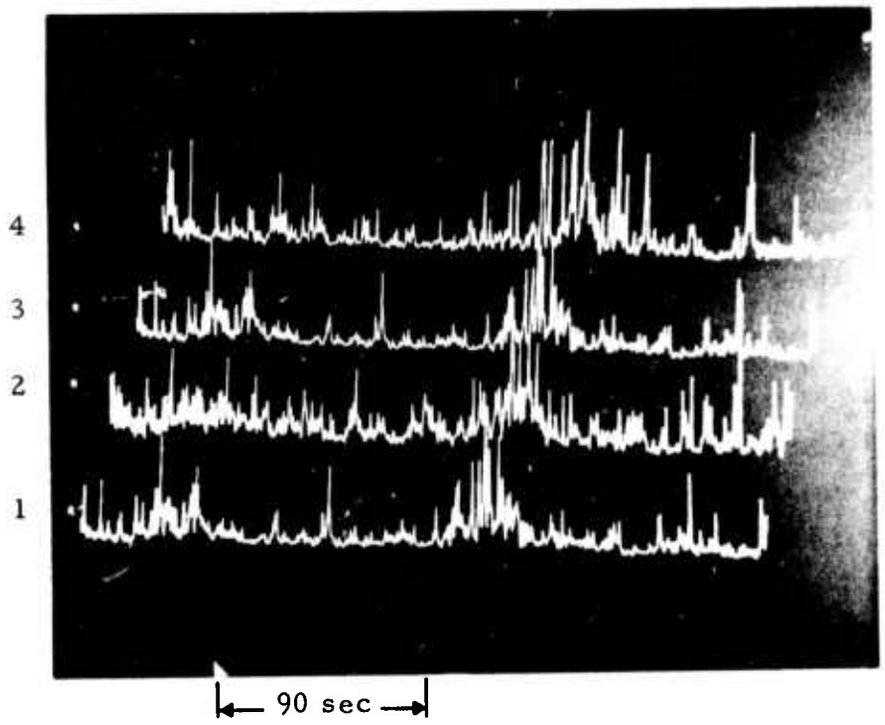

Figure 14. Squared temperature-difference fluctuations at points shown in Fig. 13b. The fluctuations are smoothed over τ = 0.4 sec. The wind speed is 3.5 m sec.

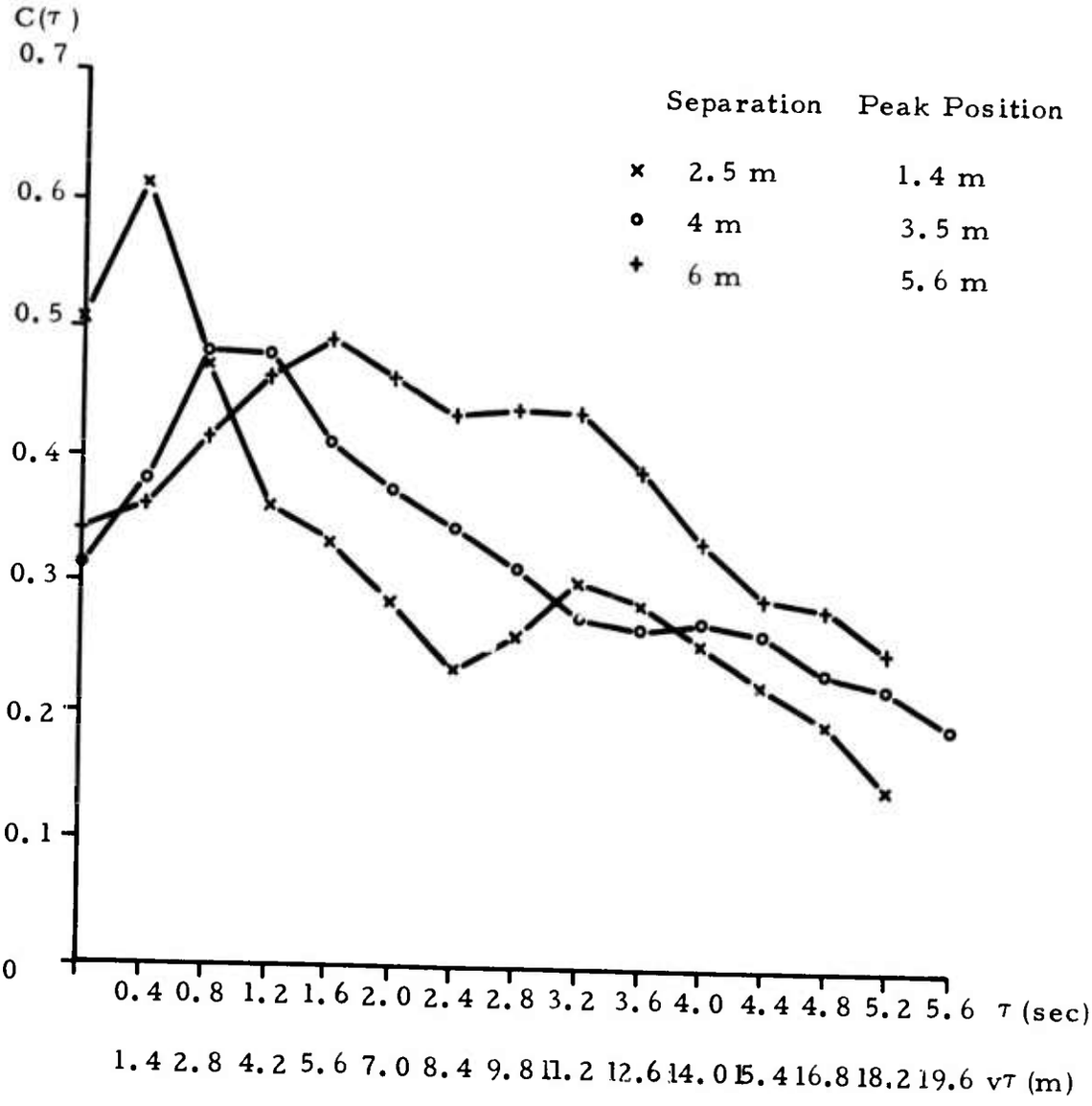

Figure 15a.
Time-lagged spatial correlation functions $C(\tau)$ for fluctuations of Fig. 14.

a. Smaller measurement-point separations
b. Larger separations.

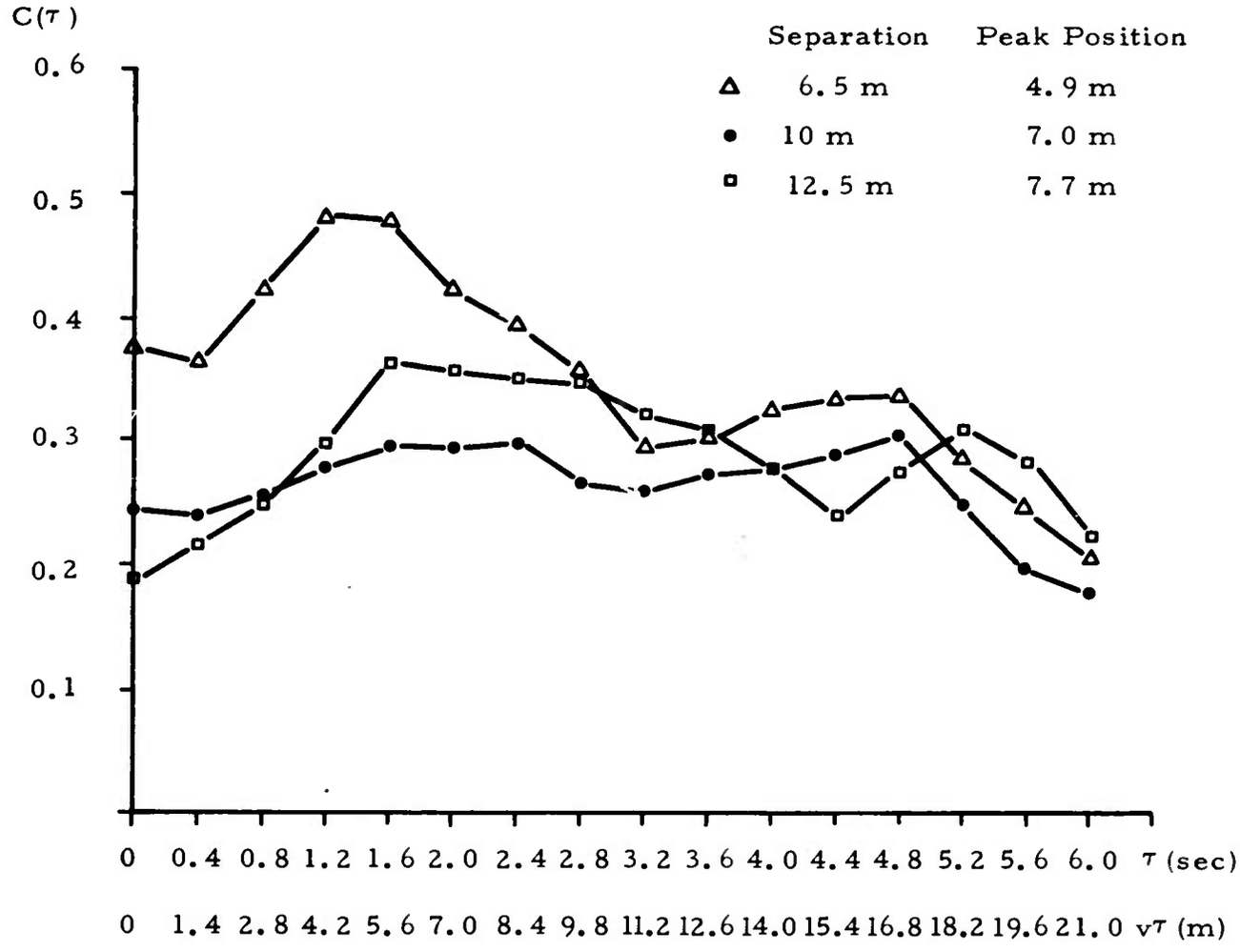
C(τ)
Separation
Peak Position
6.5 m
4.9 m
10 m
7.0 m
12.5 m
7.7 m
0.6
0.5
0.4
0.3
0.2
0.1
0 0.4 0.8 1.2 1.6 2.0 2.4 2.8 3.2 3.6 4.0 4.4 4.8 5.2 5.6 6.0 τ (sec)
0 1.4 2.8 4.2 5.6 7.0 8.4 9.8 11.2 12.6 14.0 15.4 16.8 18.2 19.6 21.0 vτ (m)

Figure 15b.

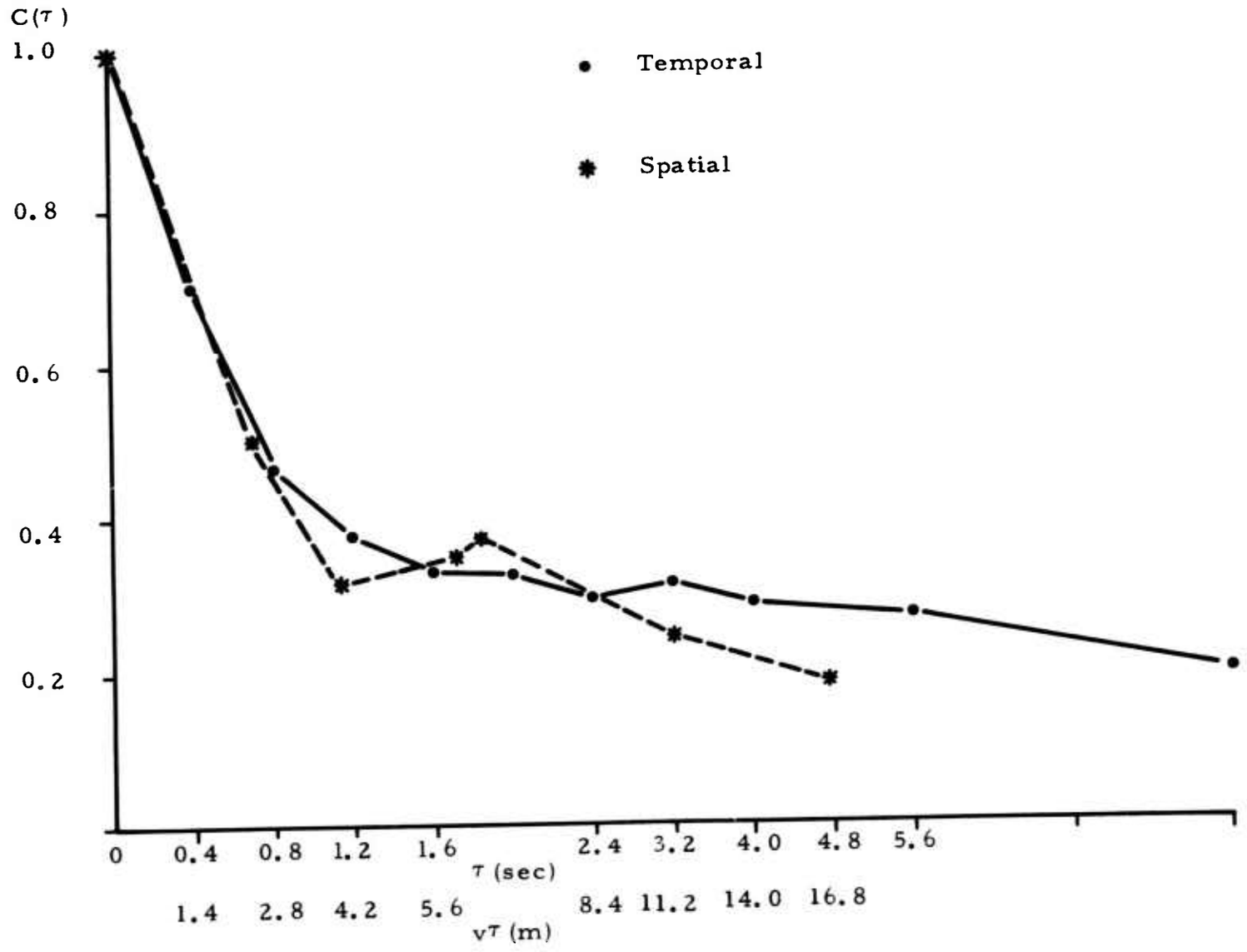

Figure 16. Comparison of spatial and temporal correlation functions $C(\tau)$ corresponding to Fig. 13b (smoothing time τ sec).

smoothing time and wind speed; in the presence of pronounced intermittency, still larger scales will predominate. Further two-dimensional experiments are being conducted.

H. Microthermal vs. Propagation Data Spread

In this section we will directly address the problem of data spread for finite averaging times, for both microthermal measurements of turbulence strength (C_n^2) and optical/infrared measurements of scintillation strength (σ^2 = log amplitude variance), and their interrelationship. We begin with purely empirical data, and then we present an analytical treatment along with preliminary data of a more sophisticated nature.

When reasonably long averaging times are used relative to the integral scales of the processes involved, one would hope for good agreement between theoretical predictions and experimental results. In Fig. 17, we show the measured log amplitude variance of scintillation vs. the value σ_T^2 as predicted by first-order theory for a uniform path:

$$\sigma_T^2 = 0.124\, C_n^2\, k^{7/6}\, L^{11/6} \quad , \tag{19}$$

where k is the optical/infrared wavenumber, L is the pathlength, and C_n^2 is determined from microthermal measurements at a point. The averaging time used for determining the abscissa and ordinate of each point was 7-10 minutes, and each two-wavelength data run was performed on a different day. The points for 10.6 microns are (with one exception) free from the effects of saturation of scintillations,[14] and very good agreement with theory is observed. These data were not specially chosen in any way, and the only requirement on the meteorological conditions was that the sky be clear or overcast in a nominally uniform manner. The points at 4880Å are of course indicative of saturation at the 1.6 km pathlength used.

In Fig. 18 we show a plot of most of the same 10.6 micron data of Fig.17, with an indication of the spread observed in short-time-averaged (10 sec) measurements of both σ_E^2 and C_n^2 or σ_T^2. The bars indicate one standard

---

14. R. S. Lawrence and J. W. Strohbehn, Proc. IEEE 58, 1523 (1970).

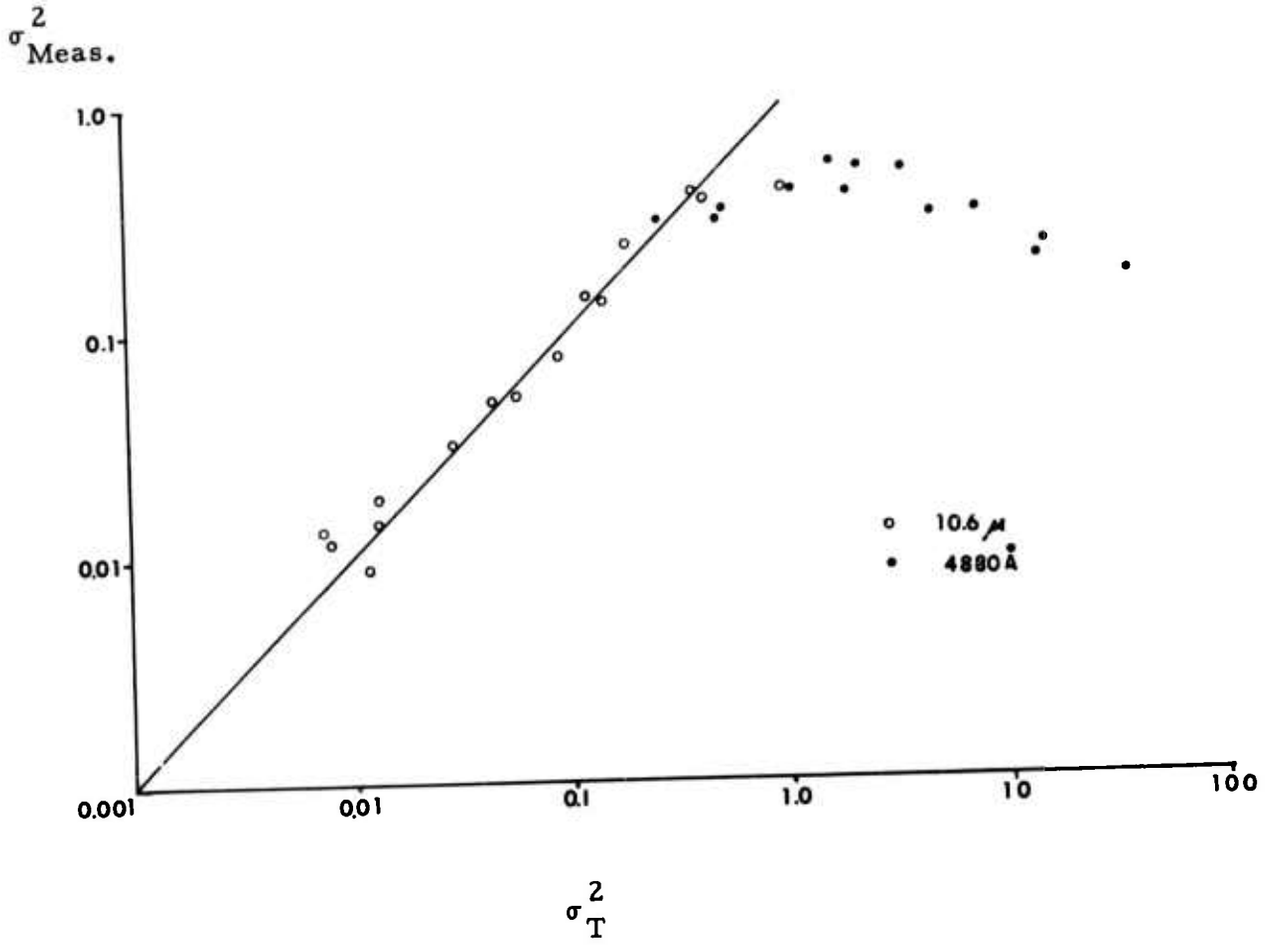

Figure 17. Experimental vs. theoretical log amplitude variance of scintillations for long averaging times.

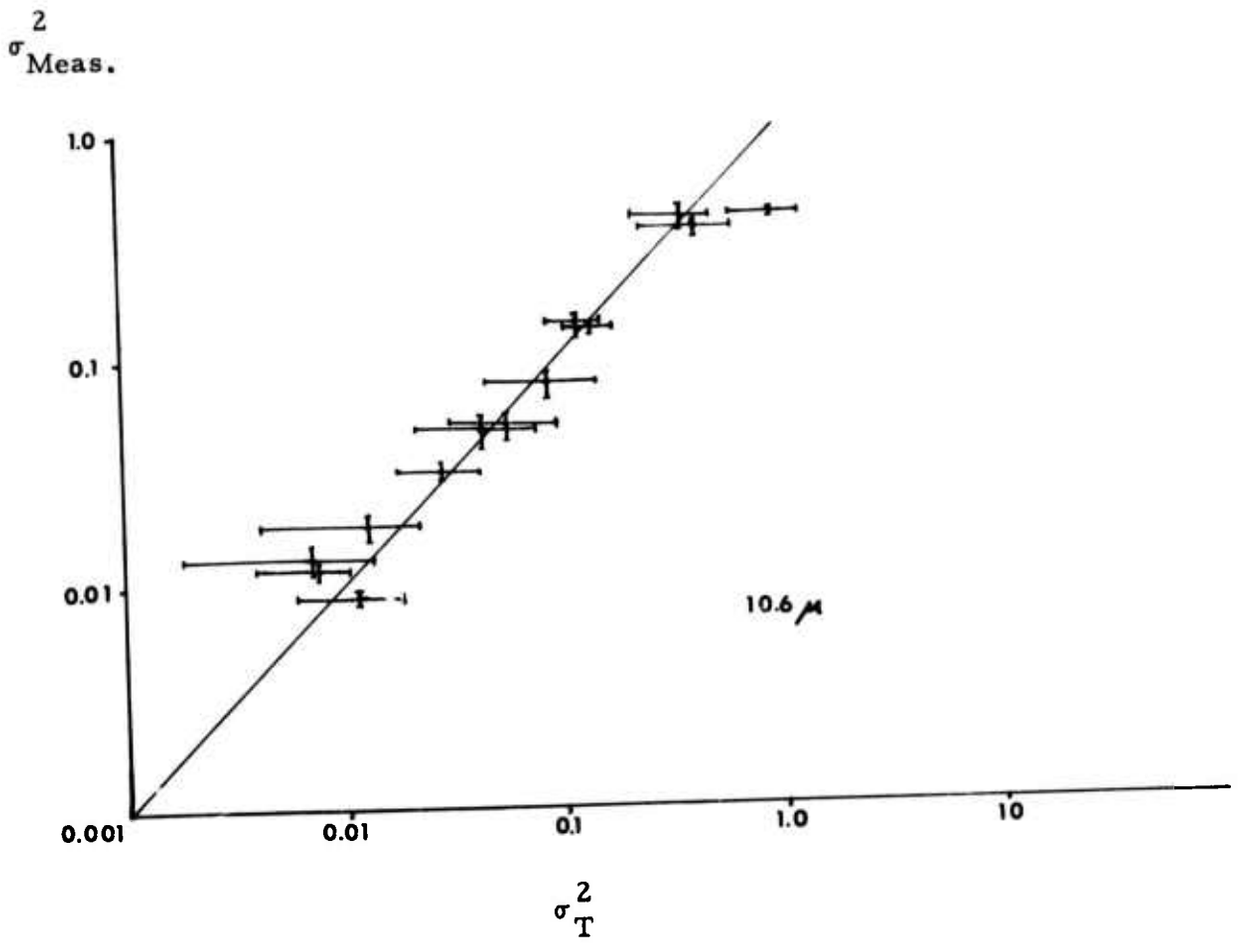

Figure 18. Optical vs. microthermal data-spread and means corresponding to 10.6 μ data of Fig. 17. The spreads indicated encompass 42-60 individual measurements, each with a 10 second averaging time.

deviation in a large number of independent 10 second measurements, crossing at the mean. We observe a much greater spread in the abscissa than the ordinate, as expected, since the former relates to a microthermal measurement at a point, while the latter relates to a propagating beam which experiences a weighted spatial average over the randomly varying turbulence strength along the path. This is also manifested in the integral scale of the squared optical/infrared amplitude (the intensity) being much smaller than that for the squared thermal fluctuations. Ordinate spreads in the saturated 4880Å regime are comparable to the unsaturated 10.6 micron spreads.

If we consider the abscissa or 10-second C_n^2 measurements alone, for this fixed averaging time we would expect the spread to tend to be inversely proportional to wind speed (v), since v determines the time scale of all of the fluctuations. This tendency is supported by the data of Fig. 19, although the degree of variability or intermittency, and its scale, are important added factors.

Let us now consider the analytical relationship between expected microthermal and optical data spread. We rewrite Eq. (19) in a form that explicitly indicates the varying nature of C_n^2 and σ^2, for any specific realization of the path:

$$\sigma_\tau^2 = \int_0^L f(z) C_{n_\tau}^2 (z)\, dz \qquad (20)$$

where f(z) is a path-weighting function dependent on optical geometry, and τ is the finite averaging time of the measurements. The viewpoint here is that the path is statistically homogeneous, and the variations indicated in Eq. (20) are simply due to the short term nature of the averages involved. We also assume stationarity and ergodicity. For a spherical wave, $f(z) \sim (z/L)^{5/6}(L-z)^{5/6}$.

In order to write this relationship, it must be assumed[15] that the turbulence strength C_n^2 varies slowly over a scale size on the order of

---

15. V. I. Tatarski, Propagation of Waves in a Turbulent Atmosphere, Nauka, Moscow, 1967.

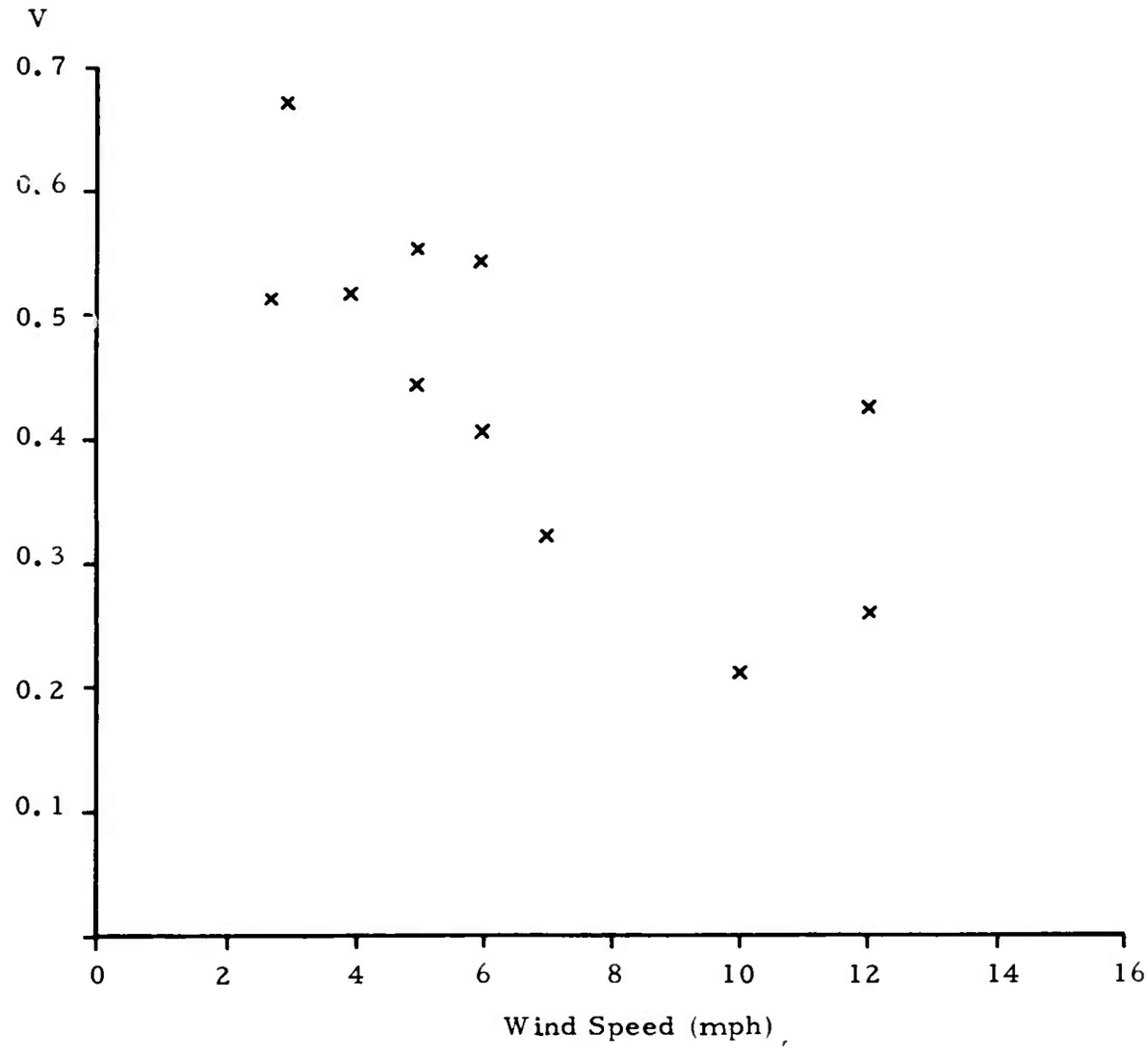

Figure 19. Normalized variance (V) of $C_{n_T}^2$ for multiple measurements as in Figure 18, vs. wind speed.

the outer scale L_o, and it is implicit that the mean-square microthermal fluctuations (or C_n^2) are z-averaged over at least a comparable scale ($\tau \geq L_o/v$). If we think of Eq. (20) as expressing the time function $\sigma_\tau^2(t)$, it is also clear that this function will not vary significantly over a time scale shorter than L_o/v, since the integral does not contain information on faster fluctuations of the scintillation strength. Of course, τ may be arbitrarily longer than this minimum value, and as it becomes very large, Eq. (20) becomes

$$\lim_{\tau \to \infty} \sigma_\tau^2 = \langle \sigma^2 \rangle = \langle C_n^2 \rangle \int_o^L f(z)dz \quad . \tag{20a}$$

However, this loses the information of interest in this discussion.

Let us now consider a series of repeated measurements of σ_τ^2 and $C_{n_\tau}^2$, the latter at any point on the statistically homogeneous path, with finite τ. The ensemble mean of a large number of such measurements will yield the same result as Eq. (20a). Of interest is the relationship between the normalized variance (data spread) in the values obtained for these two parameters. We therefore write

$$\frac{\left\langle \left(\sigma_\tau^2 - \langle \sigma^2 \rangle \right)^2 \right\rangle}{\langle \sigma^2 \rangle^2} = \frac{\int_o^L \int_o^L dz_1 dz_2 f(z_1) f(z_2) \left\langle C_{n_\tau}^2(z_1) C_{n_\tau}^2(z_2) \right\rangle}{\langle C_n^2 \rangle^2 \left(\int_o^L dz f(z) \right)^2} - 1 \tag{21}$$

It is apparent that the data spread will be determined by the <u>spatial correlation function of C_n^2 vs. z, for the averaging-time specified</u>.

We may also rewrite Eq. (21) in the form

$$\frac{\text{Var } \sigma_\tau^2}{\left\langle \sigma^2 \right\rangle^2} = \frac{\text{Var } C_{n_\tau}^{\,2}}{\left\langle C_n^{\,2} \right\rangle^2} \frac{\int_0^L dz_1 \int_0^L dz_2 \; f(z_1) f(z_2) \left(\frac{\left\langle C_{n_\tau}^{\,2}(z_1) C_{n_\tau}^{\,2}(z_2) \right\rangle - \left\langle C_n^{\,2} \right\rangle^2}{\text{Var } C_{n_\tau}^{\,2}} \right)}{\left(\int_0^L f(z) dz \right)^2} \quad . \tag{22}$$

A useful (discrete) approximation is to consider the z-correlation of $C_{n_\tau}^{\,2}$ to be either total or zero, depending on whether $|z_1 - z_2| \lesssim$ the correlation length, so that the overall correlation term on the right side of Eq. (22) is either unity or zero respectively. If we then replace the weighting function integrals with corresponding discrete summations, we have

$$\frac{\text{Var } \sigma_\tau^2}{\left\langle \sigma^2 \right\rangle^2} = \frac{\text{Var } C_{n_\tau}^{\,2}}{\left\langle C_n^{\,2} \right\rangle^2} \times \frac{\sum_{i=1}^{N} f_i^{\,2}}{\left(\sum_{i=1}^{N} f_i \right)^2} \quad , \tag{23}$$

where N is (1/2) the number of correlation lengths of $C_{n_\tau}^{\,2}$ in L. For a uniform path-weighting function, this takes the particularly simple form:

$$\frac{\text{Var } \sigma_\tau^2}{\left\langle \sigma^2 \right\rangle^2} = \frac{\text{Var } C_{n_\tau}^{\,2}}{\left\langle C_n^{\,2} \right\rangle^2} \cdot \frac{1}{N} \tag{24}$$

For a general weighting function, we may <u>define</u> the ratio of summations in Eq. (23) as N_{eq} ($\leq N$).

In order to discuss the effects of the averaging time on the optical data spread, and the relation to pertinent integral scales, we first note that the fundamental random variables related to C_n^2 and σ_τ^2 are the squared temperature fluctuations $(\Delta T)^2$ and the squared log amplitude fluctuations $(\log A - \langle \log A \rangle)^2$ respectively. The integral scale $(I_{\Delta T}^2)$ of the former may be $>> L_o$, depending on the degree of intermittency, and the integral scale of the latter will depend on the wind direction. We now distinguish two cases:

1. Wind perpendicular to the path

   In this case, the z-correlation and hence N, is unaffected by the averaging time τ. The integral scale of the squared optical fluctuations will be $I_{\Delta T}^2$, and for $\tau > I_{\Delta T}^2$, both normalized ensemble variances or data spreads in Eqs. (22-24) will be $\sim \tau^{-1}$ in accordance with Eq. (14).

   There is a subtlety leading to an apparent contradiction here. When we specify $\tau > I_{\Delta T}^2$, we are specifying that the averaging exceeds intervals over which large-scale or intermittent variations in the turbulence strength may occur. As the averaging time is increased, in accordance with Fig. 5 progressively lower frequencies, along the transverse vector, are emphasized. One may expect these frequencies or long spatial wavelengths to possess some quasi-isotropic properties, i.e. to have enlarged perpendicular- or z-correlations. This would imply that N is proportional to τ^{-1}, so that optical data spread is independent of averaging time. However, these residual, low-frequency components, even though emphasized owing to the smoothing process (τ), are <u>not</u> correlated along a direction (z) perpendicular to the smoothing.

2. Wind along the path

   In this case, if $\underline{L} > \tau > I_{\Delta T}^2$, then in accordance with the discussion of Sec. V B, the z-correlation is equal to $v\tau/2$. This assumes that the turbulence strength or envelope satisfies the "frozen-in" viewpoint. From Eq. (14), $N = L/v\tau$, and

Var $\sigma_\tau^2 / \langle \sigma_\tau^2 \rangle^2$ will be <u>independent of averaging time</u>. This manifests the fact that the integral scale of the squared optical fluctuations is on the order of L/v.

When $\tau > L/v$, we have N=1, and the optical spread will be $\sim\tau^{-1}$.

These new understandings of expected optical data spread are appropriate for experimental confirmation. The z-correlation length should be directly measured, and the microthermal and optical data spreads determined vs τ for different wind directions. Preliminary results will be discussed below. Unfortunately, the details of z-correlations of $C_n^2(z)$ will depend upon wind conditions, terrain, and turbulence and hence are not universally describable.

It is interesting to point out that, since the path-weighting function [f(z) or f_i] involves wavelength only as a multiplicative constant, the fractional spread in log amplitude variance measurements are predicted to be <u>independent of wavelength</u>. Also, note that the representation of σ_τ^2 as $\sum_{i=i}^{N} f_i C_{n_i}^2$, where the $C_{n_i}^2$ are independent, leads to the calculation of the moments of σ_τ^2 distribution from those of the $C_{n_\tau}^2$ distribution; this follows from the characteristic functions φ:

$$\varphi_{\sigma_\tau^2}(s) = \prod_{i=1}^{N} \varphi_{f_i C_{n_i}^2}(s) \tag{25}$$

where $\varphi(s)$ are the respective characteristic functions. We expect that σ_τ^2 tends to a gaussian distribution in many cases. Finally, the development leading to Eqs. (22-24) is also applicable to the case of saturated scintillations, once the appropriate weighting function (f) is known.[16]

It is apparent that, for a general wind direction, the maximum value of N is $L/v_z\tau$, and when v_z is small and/or the turbulence strength correlation region is large, N will be arbitrarily smaller than this value. In Table I, we show preliminary data of $N_{max}=L/v_z\tau$, and N approximated from Eq. (24). The wavelength was 10.6 μ, the pathlength was 1600 meters, and

---

16. H. T. Yura,"Irradiance Fluctuations of a Spherical Wave Propagating under Saturation Conditions", to be published in JOSA.

τ was 10 sec.

TABLE I

Comparison of N determined from relative optical/microthermal data spread in repeated measurements, with N_{max} determined from path-vector component of wind speed.

$C_n^2 (m^{-2/3})$	V_{Total} (m/sec)	V_z (m/sec)	N_{max}	N
1.3×10^{-14}	5.8	5.4	29.6	40.0
1.8×10^{-13}	0.8	0.8	20.0	29.6
8.3×10^{-14}	2.5	2.24	71.4	22.8
8.0×10^{-13}	1.8	1.8	88.9	61.5
1.0×10^{-13}	8.0	7.8	20.5	24.2
2.9×10^{-13}	6.0	5.0	32.0	12.1
1.9×10^{-12}	3.5	3.2	50.0	33.0
3.9×10^{-13}	1.8	1.8	88.9	80.0
1.5×10^{-14}	6.0	5.4	29.6	19.0

From this table it can be seen that the present discussion is well supported qualitatively; N exceeded N_{max} only twice. The z-correlation length (=L/2N) varied from 10 to 66 meters, and the reduction in optical data spread vs. microthermal spread ranged correspondingly from 80 to 12.

It is obviously desirable to have direct measurements of the z-correlation when the optical and microthermal spreads are compared. As of this writing, we have one reliable data sample, as given in Table II. The data relate to the signals and correlations shown in Figs. 14-16.

TABLE II.

Sample comparison of theoretical vs. experimental data spread.

Weather conditions: Clear, T=17°C, wind along path at 3.5 m/sec
$C_n^2 = 1.5 \times 10^{-14} m^{-2/3}$, $\lambda = 4880\text{Å}$
Four probe pairs spaced at z=0, 2.5, 6.5, 12.5m

1024 data points sampled at 0.4 sec intervals (6 min 50 sec total)
Relative standard deviation in C_n^2 measured from 4 respective probes=0.025
Averaging time: 0.4 sec

$$\text{Measured } \frac{\text{Var } \sigma_\tau^2}{\langle \sigma^2 \rangle^2} = 0.0306, \quad \frac{\text{Var } C_{n_\tau}^2}{\langle C_n^2 \rangle^2} = 1.99$$

Ratio = 0.0154

$$\frac{\int_0^L dz_1 \int_0^L dz_2 \, f(z_1) f(z_2) \left(\frac{\langle C_{n_\tau}^2(z_1) C_{n_\tau}^2(z_2) \rangle - \langle C_n^2 \rangle^2}{\langle C_n^2 \rangle^2} \right)}{\left(\int_0^L f(z) dz \right)^2}$$

(from Eq. 22) = 0.0115

In order to test the hypothesis that normalized data spreads are independent of wavelength, experiments were carried out over simultaneous, coincident paths of 1600 m length, at 4880Å and 1016 μ. Unfortunately, the shorter-wavelength scintillations were saturated in most conditions. The results are shown in Fig. 20.

I. Data Spread and Intermittency in Imaging Applications

Titterton [17] has raised the question of "beam breathing", related to variations in the coherence parameter ρ_o.[18] In our phenomenological theory of beam-wave effects,[18] we have not included "breathing" and see no noticeable deficiency. However, although such a variation is in principle included in any long-term or ensemble formulation of propagation problems, it would be of interest to consider the short-term behavior of ρ_o and the

---

17. Paul J. Titterton, "Beam Spread Statistics from Reciprocity", Topical Meeting on Optical Propagation through Turbulence, Boulder, Colorado, July 1974.
18. J.R.Kerr, J.R.Dunphy, "Propagation of Multiwavelength Laser Radiation Through Atmospheric Turbulence", RADC-TR-74-183, May 1974. (AD783 277)

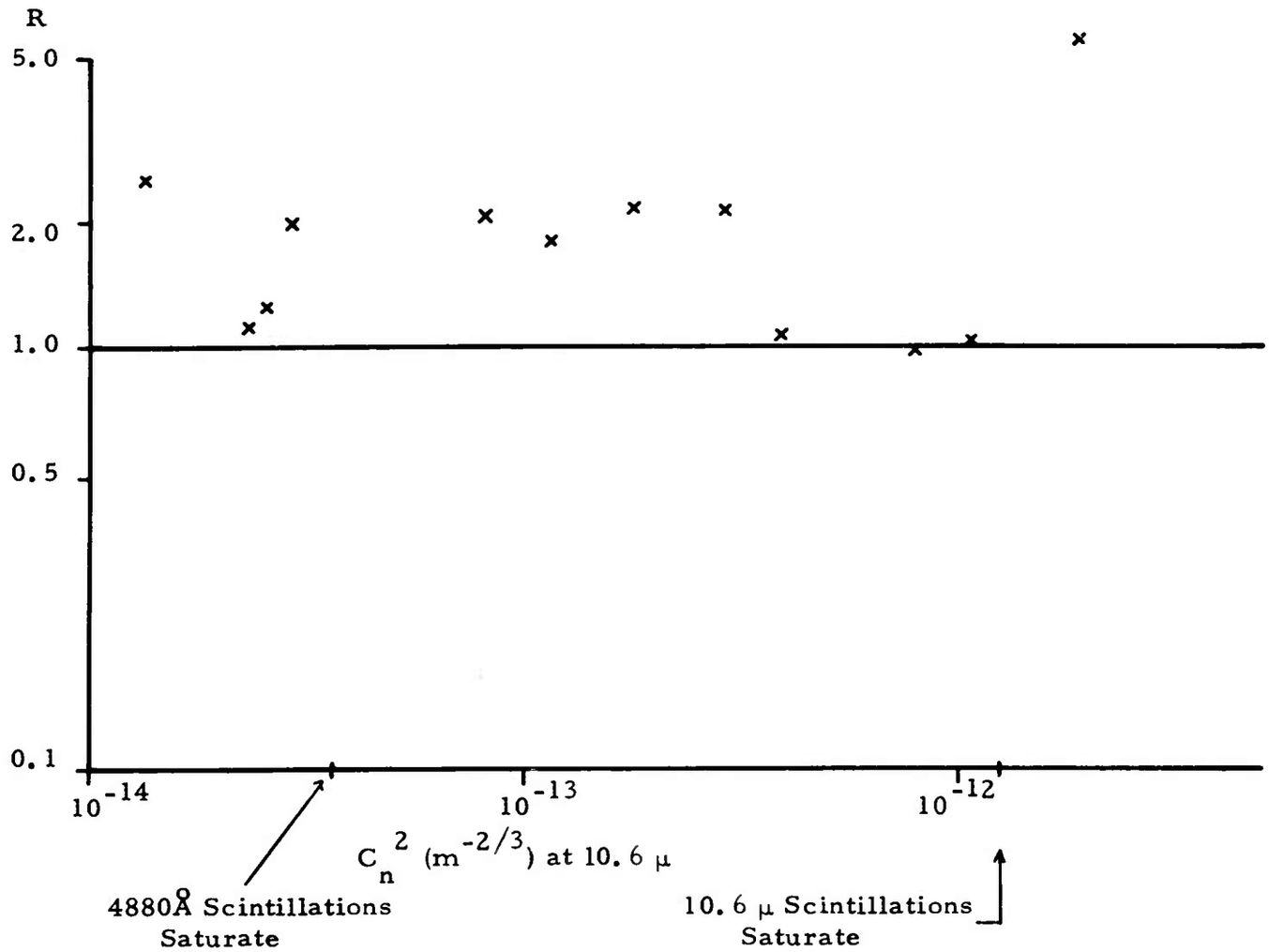

Figure 20. Ratio (R) of (normalized variance of 10 μ log amplitude variance measurements) to (normalized variance of 4880Å log amplitude variance measurements). Each point represents multiple measurements with a 10 sec averaging time per measurement.

short-term statistics of e.g. image resolution. (By "short-term" here we are not referring to quasi-instantaneous image determinations, in which image-dancing is resolved.)[18]

The dynamic behavior of ρ_o, including its probability distribution, is not described by the results of time-separated measurements; an example of the latter is in Ref. 19, in which ρ_o is seen to be log normally distributed on a day-to-day sample basis. To get at this dynamic behavior, we note that for a point source:[18]

$$\rho_o^{-5/3} = 1.45k^2 \int_o^L C_n^2(z)(z/L)^{5/3} dz \quad . \tag{26}$$

We may therefore use the methods of the preceding section, but the results will apply to the (-5/3) power of the desired variable. As a further degree of sophistication, one may utilize the so-called "short-term MTF",[18] which follows the centroid of a dancing image (i.e. removes the linear component of phase distortion). This topic comprises a possibility for future work.

III. RECENT RESULTS ON LASER ILLUMINATION THROUGH TURBULENCE

In the preceding report,[18] a comprehensive discussion was given of our current understanding of turbulence effects on finite laser beam illumination systems, including wander-cancelling systems. Also, the first set of results of an ongoing experimental effort were reported. In this section, two recent, further analytical results are presented.

A. Effective Aperture for a Truncated Gaussian Transmitter

As discussed in Ref. 18, the results for the mean on-axis target irradiance for a focused beam propagating through turbulence, with and without wander cancellation, can be expressed universally in terms of the ratio D/ρ_o as an independent variable. The parameter D is some measure of the transmitter diameter, and ρ_o is the point-source coherence length over the reciprocal path (i.e., from target to transmitter). We explicitly considered both a uniform circular aperture, and a nontruncated gaussian aperture, and found that the results are practically the same in both cases once the proper comparative abscissas (effective diameters) have

---

19. D.L.Fried and G.E.Mevers, "Evaluation of r_o for Propagation Down Through the Atmosphere", preprint, Nov. 1973.

been established. It is then reasonable to expect that these results will also apply to the practical case of a truncated gaussian transmitter; the purpose of this section is to derive the appropriate measure of diameter of the beam for the general case of arbitrary truncation.

To do this, we write

$$I(\alpha) \propto \int_0^\infty dx \; x \; f(x) e^{-(\alpha x)^{5/3}} \tag{27}$$

which is obtained from the Huygens-Fresnel formulation.[18] Our notation, which is slightly changed from Ref. 18, is as follows:

D_g = 2a = 1/e diameter of gaussian intensity distribution at transmitter

D = physical diameter of truncation aperture

$x = \rho/D_g$ = normalized difference-coordinate in transmitter plane

$\alpha = D_g/\rho_o$

The function f(x) is from the overlap integral for the particular distribution of illumination over the aperture. Although the above expression could be worked out rigorously for each value of D/D_g, the near coincidence of non-truncated-gaussian and uniform-illumination cases suggests that we need merely define an appropriate "effective diameter" for the general case.

To do this, we note from Ref. 18 that the effective diameter (D_{eff}) for both the uniform case and the nontruncated gaussian case is specified by the ratio of the limits:

$$\frac{I_\infty}{I_o} \equiv \frac{\lim_{\alpha\to\infty} I(\alpha)}{\lim_{\alpha\to 0} I(\alpha)} = \frac{r_o^2}{D_{eff}^2} = \frac{(2.0986\rho_o)^2}{D_{eff}^2} \quad , \tag{28}$$

where D_{eff}=D and $2D_g$ for the two cases respectively. For the general case, we define

$$\eta = \frac{D^2}{D_g^2}$$

Then from the truncated-beam-wave diffraction theory in a vacuum,[20] we write

$$I_o = \frac{U_o^2 k^2}{L^2} \frac{D_g^4}{16} (1-e^{-\eta/2})^2 \tag{29}$$

where U_o is the transmitter amplitude on beam axis. We note that, from simple integration, the transmitter power P is given by

$$P = \frac{D_g^2 \pi}{4} U_o^2 (1-e^{-\eta}) \tag{30}$$

For the nontruncated case, we can write[18]

$$I_\infty = \frac{U_o^2 k^2}{L^2} \frac{D_g^2 r_o^2}{64} \tag{31}$$

We know that I_∞/P is controlled by the turbulence, and thus for the truncated case this ratio must be independent of D, D_g. It is thus apparent dimensionally that for the general case,

$$I_\infty = \frac{U_o^2 k^2}{L^2} \frac{D_g^2 r_o^2}{64} (1-e^{-\eta}) \tag{32}$$

As a check, we note that this approaches the correct limit[18] when $\eta \to 0$.

---

20. G. Olaofe, J. Opt. Soc. Am. 60, 1654 (1970).

We now take the Ratio of Eqs. (32) and (29), and combine with (28), to write

$$D_{eff} = 2D_g \left(\frac{1-e^{-\eta/2}}{\sqrt{1-e^{-\eta}}} \right) \quad . \tag{33}$$

The ratio $D_{eff}/2D_g$ is plotted in Fig. 21. These results will be used in the future to unify all presentations of data. They may also be used as an approximation to the effective aperture for a truncated gaussian beam, when second moment or irradiance fading data are presented.

Finally, we note that the phenomenological theory given in Ref. 18 can be written in terms of r_o, D_{eff} instead of ρ_o, D_g, with a resulting simplification in the numerical constants. This will be done in a forthcoming publication based on that report.

B. Limit of Irradiance Variance at Large Values of D/ρ_o

In the previous report,[18] it was pointed out that both the phenomenological model and experimental data suggest that the normalized irradiance variance for a transmitter much larger than the coherence scale must approach unity. Through reciprocity, this would also be true of a large heterodyne reciever. Although this seems to be clearly necessary physically, it disagrees with earlier approximate analyses of heterodyne systems.[21] The point of the present section is to derive this limit directly from the Huygens-Fresnel expression for the second moment of irradiance (fourth moment of amplitude).

The required Huygens-Fresnel expression is given in Ref. 22. For a nontruncated gaussian beam, this may be readily reduced to the eight-fold integral:

---

21. D. L. Fried, "Effects of Atmospheric Turbulence on Static and Tracking Optical Heterodyne Receivers/Average Gain and Antenna Gain Variation", Technical Report No. TR-027, Optical Science Consultants, August 1971.
22. H. T. Yura, Applied Optics 11, 1399-1406, June 1972.

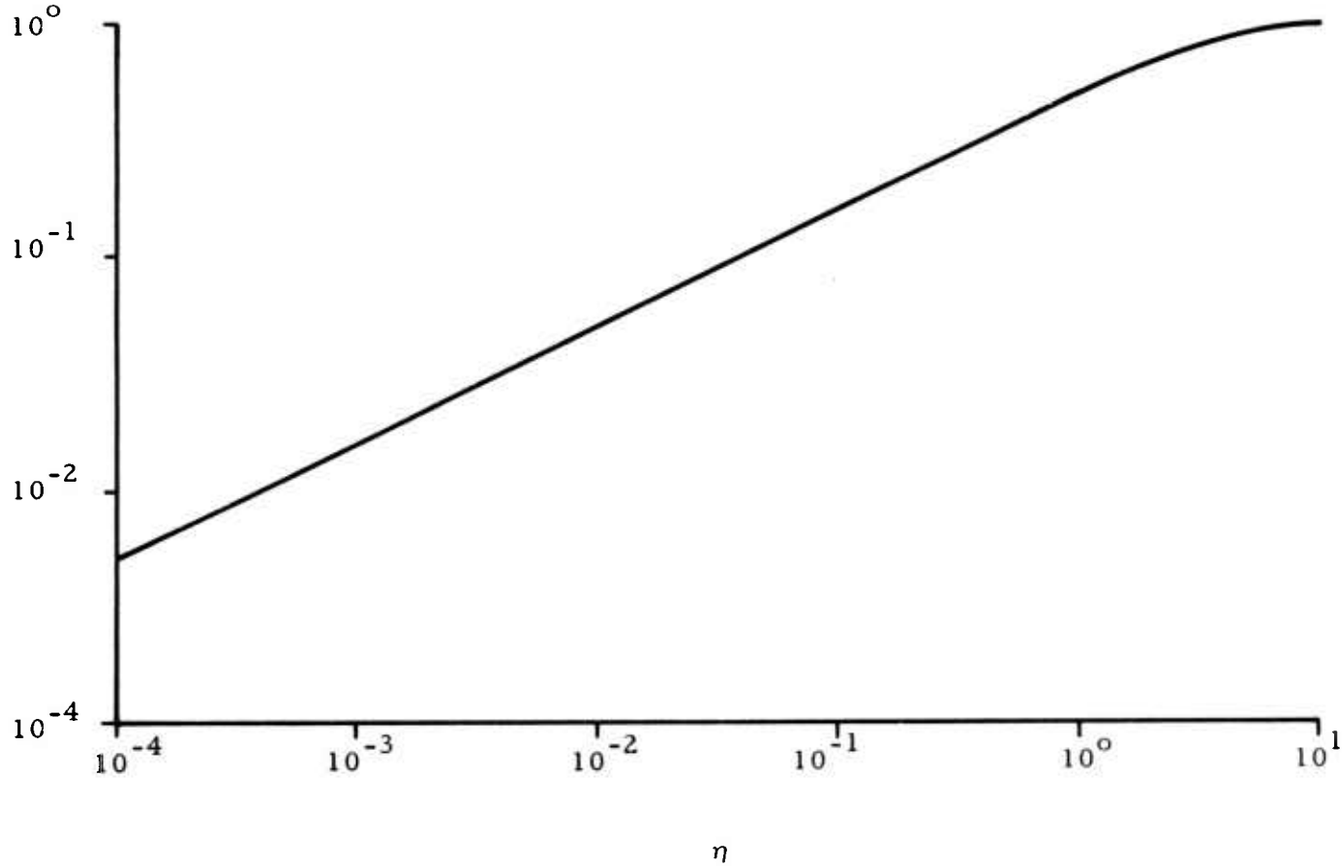

Figure 21. Ratio of $\frac{D_{eff}}{2\ Dg}$ vs. η from Eq. (33).

$$\langle I^2 \rangle = \left(\frac{k}{2\pi L}\right)^4 \iiint\!\!\iint d\vec{\rho}_1\, d\vec{\rho}_2\, d\vec{\rho}_3\, d\vec{\rho}_4 \quad \exp\left\{ - \frac{\rho_1^2+\rho_2^2+\rho_3^2+\rho_4^2}{D_g} \right\}$$

$$\cdot \exp\left\{ -\left(\frac{D_g}{\rho_o}\right)^{5/3} \frac{1}{D_g^{5/3}} \left[|\vec{\rho}_1-\vec{\rho}_2|^{5/3} + |\vec{\rho}_3-\vec{\rho}_4|^{5/3} + |\vec{\rho}_1-\vec{\rho}_4|^{5/3} \right.\right.$$

$$\left.\left. + |\vec{\rho}_2-\vec{\rho}_3|^{5/3} - |\vec{\rho}_2-\vec{\rho}_4|^{5/3} - |\vec{\rho}_1-\vec{\rho}_3|^{5/3} \right] \right\}$$

$$\cdot \exp\left\{ C_\ell(|\vec{\rho}_1-\vec{\rho}_3|) + C_\ell(|\vec{\rho}_2-\vec{\rho}_4|) \right\} \qquad (34)$$

where D_g is the $\frac{1}{e}$ irradiance diameter, $\vec{\rho}$ is the i^{th} difference-vector in the transmitter plane, and C_ℓ is the log amplitude covariance function. It may be shown from physical reasoning,[21] or from tedious but straightforward analytical calculations, that the covariance functions may be dropped* when we consider the limit $D_g/\rho_o \to \infty$.

---

*It may also be shown that this is equivalent to dropping the amplitude term in the perturbation Green's function, as done in Ref. 23. In the latter effort, the phase perturbation was assumed to be gaussian, and the problem under discussion here was reduced to a six-fold integral for numerical evaluation. Although the results in the limit of large D_g/ρ_o agree with those presented here, it may be demonstrated that the dropping of the amplitude term results in inaccuracies at smaller values of D_g/ρ_o.

We let $x = \rho/D_g$, $\alpha = \frac{D_g}{\rho_o}$, and write (34) as

$$\langle I^2 \rangle = \left(\frac{kD_g}{2\pi L}\right)^4 \iiint\!\!\iint d\vec{x}_1 d\vec{x}_2 d\vec{x}_3 d\vec{x}_4 \quad \exp\left\{ -\left(x_1^2+x_2^2+x_3^2+x_4^2\right) \right\}$$

---

23. V. A. Banakh, et al, J. Opt. Soc. Am. 64, 516-518, April 1974.

$$\cdot\exp\left\{-(\alpha)^{5/3}\left[|\vec{x}_1-\vec{x}_2|^{5/3}+|\vec{x}_3-\vec{x}_4|^{5/3}+|\vec{x}_1-\vec{x}_4|^{5/3}+|\vec{x}_2-\vec{x}_3|^{5/3}\right.\right.$$
$$\left.\left.-|\vec{x}_2-\vec{x}_4|^{5/3}-|\vec{x}_1-\vec{x}_3|^{5/3}\right]\right\} \tag{35}$$

We now write

$$\lim_{\alpha\to\infty}\exp\left\{-(\alpha)^{5/3}\left[|\vec{x}_1-\vec{x}_2|^{5/3}+|\vec{x}_1-\vec{x}_4|^{5/3}\right]\right\}$$
$$=6/5\pi\Gamma(6/5)(\alpha)^{-2}\exp\left\{-(\alpha)^{5/3}|\vec{x}_1-\vec{x}_4|^{5/3}\right\}\delta(|x_1-x_2|)$$
$$+6/5\pi\Gamma(6/5)(\alpha)^{-2}\exp\left\{-(\alpha)^{5/3}|\vec{x}_1-\vec{x}_2|^{5/3}\right\}\delta(|\vec{x}_1-\vec{x}_4|) \tag{36}$$

i.e. $$\delta(|\vec{x}_1-\vec{x}_2|)=\lim_{\alpha\to\infty}5/6\ \frac{\alpha^2}{\pi\Gamma(6/5)}\ \exp\left\{-(\alpha)^{5/3}|\vec{x}_1-\vec{x}_2|^{5/3}\right\} \tag{37}$$

where we note that this satisfies the properties of a delta function:

$$\int_{-\infty}^{\infty}\delta(|\vec{x}_1-\vec{x}_2|)\,dx_1=1$$

$$\lim_{\vec{x}_1\to\vec{x}_2}\delta(|\vec{x}_1-\vec{x}_2|)=\lim_{\alpha\to\infty}5/6\ \frac{\alpha^2}{\pi\Gamma(6/5)}\to\infty$$

$$\delta(|\vec{x}_1-\vec{x}_2|)\Big|_{\vec{x}_1\neq\vec{x}_2}=\lim_{\alpha\to\infty}5/6\ \frac{\alpha^2}{\pi\Gamma(6/5)}\ \exp\left\{-(\alpha)^{5/3}\Delta\right\}=0$$

Using (36) with (35), we have

$$\lim_{\alpha\to\infty}\left\langle I^2\right\rangle=\left(\frac{kD_g}{2\pi L}\right)^4(6/5)\ \frac{\pi\Gamma(6/5)}{\alpha^2}\left\{\iiint d\vec{x}_2d\vec{x}_3d\vec{x}_4\ \exp\left[-(2x_2^2+x_3^2+x_4^2)\right]\right.$$
$$\exp\left[-(\alpha)^{5/3}\ (\vec{x}_3-\vec{x}_4)^{5/3}\right]+\iiint d\vec{x}_2d\vec{x}_3d\vec{x}_4\ \exp\left[-(x_2^2+x_3^2+2x_4^2)\right]$$
$$\left.\exp\left[-(\alpha)^{5/3}\ (\vec{x}_2-\vec{x}_3)^{5/3}\right]\right\} \tag{38}$$

Iterating this procedure for the term in each of the integrands of the form $\exp\left\{-(\alpha)^{5/3}\ |\vec{x}_i-\vec{x}_j|^{5/3}\right\}\Rightarrow 6/5\pi\Gamma(6/5)\alpha^{-2}\ \delta(|\vec{x}_i-\vec{x}_j|)$ results in

$$\lim_{\alpha\to\infty} \left\langle I^2 \right\rangle = \left(\frac{kD_g}{2\pi L}\right)^4 \left[(6/5)\frac{\pi\Gamma(6/5)}{\alpha^2}\right]^2 \left\{ \iint d\vec{x}_2 d\vec{x}_4 \exp\left[-2(x_2^2+x_4^2)\right] + \iint d\vec{x}_3 d\vec{x}_4 \exp\left[-2(x_3^2+x_4^2)\right] \right\} \tag{39}$$

$$\lim_{\alpha\to\infty} \left\langle I^2 \right\rangle = \left(\frac{kD_g}{2\pi L}\right)^4 (3/5)^2 \frac{(2\pi)^2\Gamma^2(6/5)}{\alpha^4} (\pi/2)^2(2)$$

$$= \left(\frac{kD_g}{2L}\right)^4 (3/5)^2 \frac{\Gamma^2(6/5)}{8}$$

$$= .0379\left(\frac{kD_g}{2L}\right)^4 \tag{40}$$

Similarly, we may write

$$\lim_{\alpha\to\infty} \left\langle I \right\rangle = \left(\frac{kD_g}{2\pi L}\right)^2 \iint d\vec{x}_1 d\vec{x}_2 \exp -\left\{\frac{x_1^2+x_2^2}{2}\right\} .\exp\left\{-\alpha^{5/3} |\vec{x}_1-\vec{x}_2|^{5/3}\right\} \tag{41}$$

Using the delta function, this becomes

$$\lim_{\alpha\to\infty} \left\langle I \right\rangle = \left(\frac{kD_g}{2\pi L}\right)^2 (3/5) \frac{2\pi\Gamma(6/5)}{\alpha^2} \int d\vec{x}_2 e^{-2\vec{x}_2^2}$$

$$= \left(\frac{kD_g}{L\alpha}\right)^2 (3/5) \frac{\Gamma(6/5)}{4}$$

$$= 0.1377\left(\frac{kD_g}{L\alpha}\right)^2 \tag{42}$$

Finally, we write from (40) and (42):

$$\lim_{\alpha\to\infty} \sigma_I^2 = \frac{\left\langle I_\infty^2 \right\rangle - \left\langle I_\infty \right\rangle^2}{\left\langle I_\infty \right\rangle^2} = 1 \quad .$$

This is the desired result.*

---

*In order to make the development of the present section agree with that of Ref. 18, it is necessary to multiply I by $\frac{4}{\pi} U_o^2 D_g^2$.

IV. FUTURE WORK

In a follow-on effort, we will obtain more complete experimental results on short-term statistical effects, using the analytical understandings presented in Sec. II, and we will carry out related computer simulation work.

Comprehensive experiments on finite-beam target illumination effects will be completed, with varying pathlengths and wavelengths. In addition, our recent analytical advances in the rigorous determination of the second moment of irradiance vs. D/ρ_o will be pursued, with supporting numerical calculations.

V. REFERENCES

1. J. R. Kerr, "Propagation of Multiwavelength Laser Radiation Through Atmospheric Turbulence", RADC-TR-73-322, August, 1973. (AD769 /92)
2. A. M. Yaglom, Soviet Physics-Doklady 11, 26-29, July 1966.
3. A. S. Gurvich and A. M. Yaglom, Phys. of Fluids Suppl., Boundary Layers and Turbulence, 10, Part II, S59-S65 (1967).
4. G. J. Hahn and S. S. Shapiro, Statistical Models in Engineering, Wiley & Sons, 197 (1967).
5. H. Tennekes, J. C. Wyngaard, J. Fluid Mech. 55, 93-103 (1972).
6. J. L. Lumley, "Stochastic Tools in Turbulence", Acad. Pr., 1970.
7. S. A. Collins and G. W. Reinhardt, "Investigation of Laser Propagation Phenomena", RADC-TR-71-248, August 1971, Electroscience Laboratory, Ohio State University. (AD734 547)
8. R. S. Lawrence, G. R. Ochs, S. F. Clifford, J. Opt. Soc. Am. 60, 826 (1970).
9. G. J. Hahn and S. S. Shapiro, Statistical Models in Engineering, Wiley and Sons, 1967.
10. Benoit Mandelbrot, "Intermittent Turbulence in Self Similar Cascades", J. Fluid Mechanics, 62, Part II, 331-358 (1974).
11. A. M. Yaglom, An Introduction to the Theory of Stationary Random Functions, Prentice-Hall, 1962.
12. J. L. Doob, Stochastic Processes, Wiley & Sons, 1953.
13. A. Papoulis, Probability Random Variables and Stochastic Processes, McGraw-Hill, 1965.
14. R. S. Lawrence and J. W. Strohbehn, Proc. IEEE 58, 1523 (1970).
15. V. I. Tatarski, Propagation of Waves in a Turbulent Atmosphere, Nauka, Moscow, 1967.
16. H. T. Yura, "Irradiance Fluctuations of a Spherical Wave Propagating under Saturation Conditions", to be published in JOSA.
17. Paul J. Titterton, "Beam Spread Statistics from Reciprocity", Topical Meeting on Optical Propagation Through Turbulence, Boulder, Colorado, July 1974.
18. J. R. Kerr, J. R. Dunphy, "Propagation of Multiwavelength Laser Radiation Through Atmospheric Turbulence", RADC-TR-74-183, May 1974.
19. D. L. Fried and G. E. Mevers, "Evaluation of r_o for Propagation Down Through the Atmosphere", preprint, Nov. 1973. (AD783 277)
20. G. Olaofe, J. Opt. Soc. Am. 60, 1654 (1970).
21. D. L. Fried, "Effects of Atmospheric Turbulence on Static and Tracking Optical Heterodyne Receivers/Average Gain and Antenna Gain Variation", Technical Report No. TR-027, Optical Science Consultants, August 1971.
22. H. T. Yura, Applied Optics 11, 1399-1406, June 1972.
23. V. A. Banakh, et al, J. Opt. Soc. Am. 64, 516-518, April 1974.

MISSION
of
Rome Air Development Center

RADC is the principal AFSC organization charged with planning and executing the USAF exploratory and advanced development programs for electromagnetic intelligence techniques, reliability and compatibility techniques for electronic systems, electromagnetic transmission and reception, ground based surveillance, ground communications, information displays and information processing. This Center provides technical or management assistance in support of studies, analyses, development planning activities, acquisition, test, evaluation, modification, and operation of aerospace systems and related equipment.

Source AFSCR 23-50, 11 May 70